RADON-HAZARD-POTENTIAL AREAS IN SANDY, SALT LAKE COUNTY, AND PROVO, UTAH COUNTY, UTAH

by
Barry J. Solomon, Bill D. Black
Dennis L. Nielson
Dane L. Finerfrock, John D. Hultquist
Cui Linpei

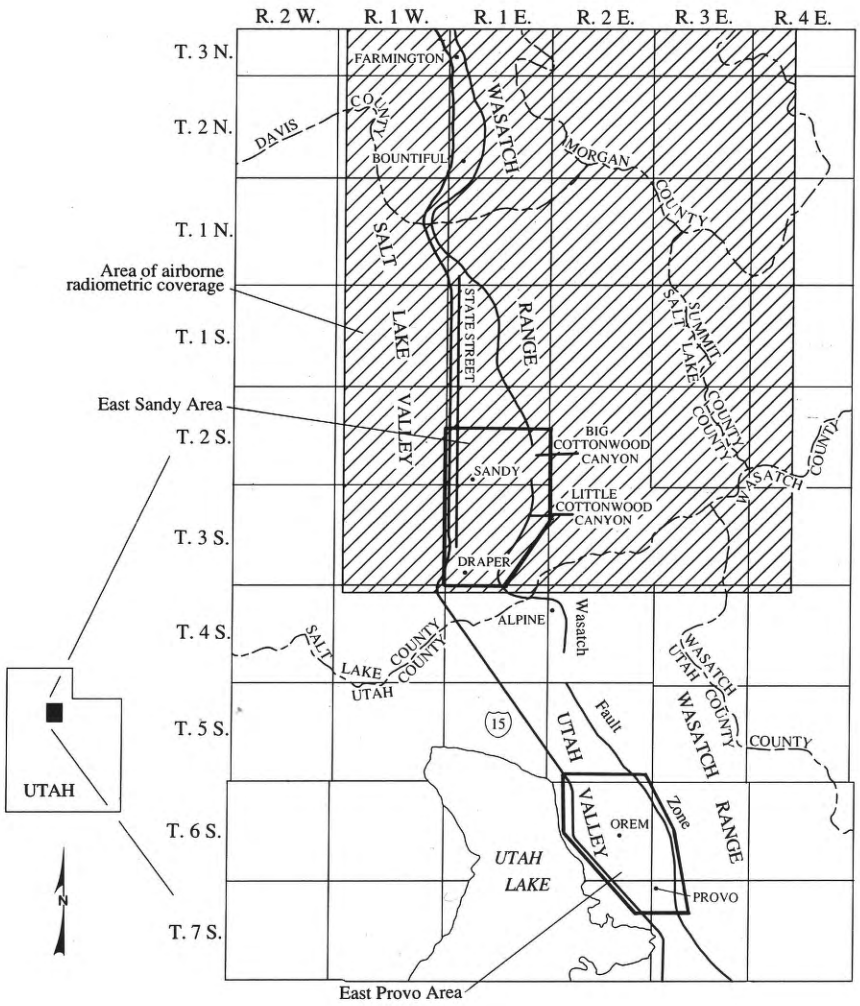

Special Study 85 **1994**
UTAH GEOLOGICAL SURVEY
a division of
UTAH DEPARTMENT OF NATURAL RESOURCES
in cooperation with
U.S. ENVIRONMENTAL PROTECTION AGENCY

UTAH GEOLOGICAL SURVEY
2363 South Foothill Drive
Salt Lake City, Utah 84109-1491
Phone: (801) 467-7970 Fax: (801) 467-4070

THE UTAH GEOLOGICAL SURVEY is organized into three geologic programs with Administration, Editorial, and Computer Resources providing necessary support to the programs. THE ECONOMIC GEOLOGY PROGRAM undertakes studies to identify coal, geothermal, uranium, hydrocarbon, and industrial and metallic mineral resources; to initiate detailed studies of the above resources including mining district and field studies; to develop computerized resource data bases, to answer state, federal, and industry requests for information; and to encourage the prudent development of Utah's geologic resources. THE APPLIED GEOLOGY PROGRAM responds to requests from local and state governmental entities for engineering geologic investigations; and identifies, documents, and interprets Utah's geologic hazards. THE GEOLOGIC MAPPING PROGRAM maps the bedrock and surficial geology of the state at a regional scale by county and at a more detailed scale by quadrangle. The Geologic Extension Service answers inquiries from the public and provides information about Utah's geology in a non-technical format.

The UGS manages a library which is open to the public and contains many reference works on Utah geology and many unpublished documents on aspects of Utah geology by UGS staff and others. The UGS has begun several computer data bases with information on mineral and energy resources, geologic hazards, stratigraphic sections, and bibliographic references. Most files may be viewed by using the UGS Library. The UGS also manages a sample library which contains core, cuttings, and soil samples from mineral and petroleum drill holes and engineering geology investigations. Samples may be viewed at the Sample Library or requested as a loan for outside study.

The UGS publishes the results of its investigations in the form of maps, reports, and compilations of data that are accessible to the public. For information on UGS publications, contact the Sales Office, 2363 South Foothill Drive, Salt Lake City, Utah 84109-1491, (801) 467-0401.

RADON-HAZARD-POTENTIAL AREAS IN SANDY, SALT LAKE COUNTY, AND PROVO, UTAH COUNTY, UTAH

by
Barry J. Solomon, Bill D. Black
Dennis L. Nielson
Dane L. Finerfrock, John D. Hultquist
Cui Linpei

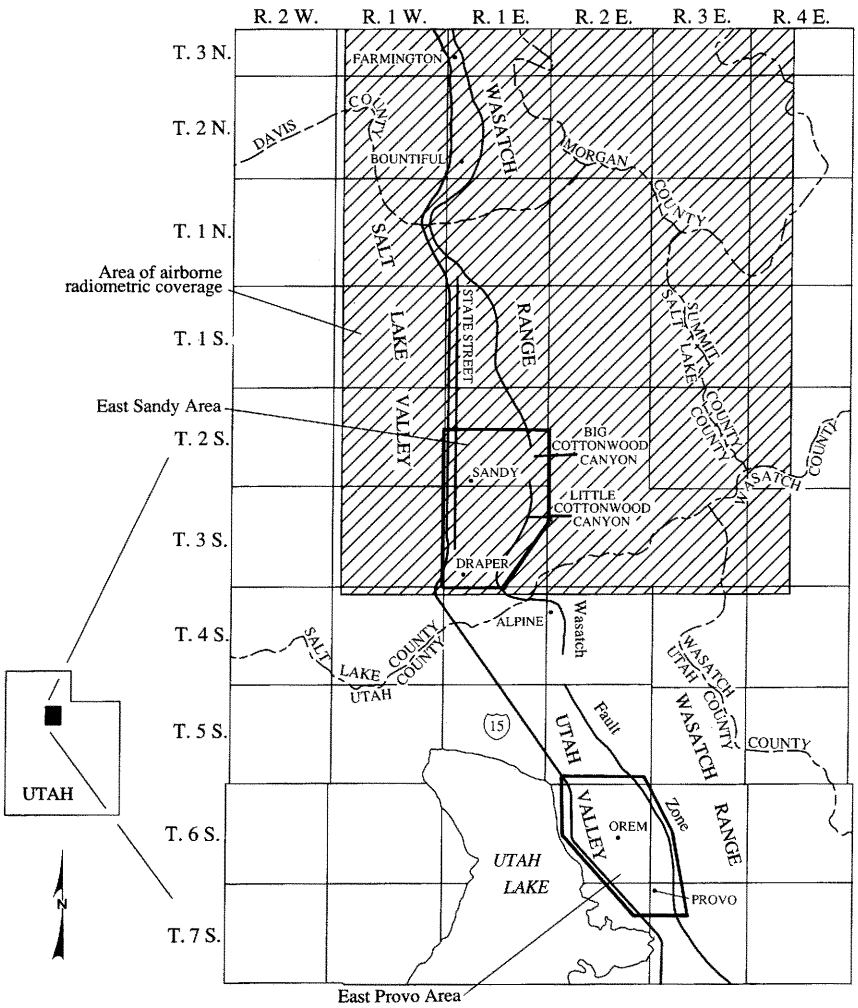

Special Study 85 **1994**
UTAH GEOLOGICAL SURVEY
a division of
UTAH DEPARTMENT OF NATURAL RESOURCES
in cooperation with
U.S. ENVIRONMENTAL PROTECTION AGENCY

RADON-HAZARD-POTENTIAL AREAS IN SANDY, SALT LAKE COUNTY, AND PROVO, UTAH COUNTY, UTAH

by

Barry J. Solomon and Bill D. Black
Utah Geological Survey
2363 South Foothill Drive, Salt Lake City, Utah 84109-1491

Dennis L. Nielson
University of Utah Research Institute
391-C Chipeta Way, Salt Lake City, Utah 84108

Dane L. Finerfrock and John D. Hultquist
Utah Department of Environmental Quality
Division of Radiation Control
168 North 1950 West, Salt Lake City, Utah 84114-4850

Cui Linpei
Institute of Geological Information
Beijing, People's Republic of China

FIRST-YEAR GEOLOGIC STUDIES FOR THE
U.S. ENVIRONMENTAL PROTECTION AGENCY
STATE INDOOR RADON GRANT PROGRAM

Reference herein to any specific commercial product, process, or service by trade name, trademark, manufacturer, or otherwise, does not necessarily constitute or imply its endorsement, recommendation, or favoring by the Utah Geological Survey or the U.S. Environmental Protection Agency. The views and opinions of authors expressed herein do not necessarily state or reflect those of the U.S. Environmental Protection Agency.

CONTENTS

FIGURES

TABLES

RADON-HAZARD-POTENTIAL AREAS IN SANDY, SALT LAKE COUNTY, AND PROVO, UTAH COUNTY, UTAH

Barry J. Solomon and Bill D. Black
Utah Geological Survey
2363 South Foothill Drive, Salt Lake City, Utah 84109-1491

Dennis L. Nielson
University of Utah Research Institute
391-C Chipeta Way, Salt Lake City, Utah 84108

Dane L. Finerfrock and John D. Hultquist
Utah Department of Environmental Quality
Division of Radiation Control
168 North 1950 West, Salt Lake City, Utah 84114-4850

Cui Linpei
Institute of Geological Information
Beijing, People's Republic of China

ABSTRACT

Average indoor-radon levels in two areas of the Wasatch Front region of north-central Utah are considerably higher than the national average of 1.7 picocuries per liter (pCi/L) (63 Becquerels per cubic meter [Bq/m^3]). The average indoor-radon level on the east bench of Sandy near Little Cottonwood Canyon is 3.8 pCi/L (141 Bq/m^3) and on the east bench of Provo it is 2.9 pCi/L (107 Bq/m^3). However, indoor measurements are affected by construction type, building maintenance, occupant lifestyle, and weather and cannot be used to accurately estimate the radon-hazard potential in nearby, untested homes. Geologic characteristics of foundation materials which govern the potential for indoor radon are relatively uniform within geologic units that underlie the study areas, and were used to estimate the radon-hazard potential of Sandy and Provo.

The radon-hazard potential was estimated using three geologic factors: (1) uranium content of soils, (2) concentration of radon in soil gas, and (3) depth to ground water. Numerical scores were applied to each factor, and three radon-hazard-potential categories were established based on the cumulative totals of the three factors. The categories characterize the hazard potential of each major Quaternary geologic unit.

Geologic units with the highest potential for elevated indoor-radon concentrations are upper Pleistocene lacustrine deposits related to the transgressive phase of the Bonneville lake cycle, younger alluvial and colluvial deposits overlying the transgressive lacustrine units, and older, middle and upper Pleistocene glacial deposits. Well-drained, regressive-phase alluvium deposited on deltas on the margin of Lake Bonneville predominate. At the mouth of Little Cottonwood Canyon in east Sandy this alluvium contains abundant detritus from Tertiary granitic stocks and has high concentrations of both uranium (averaging 6.9 parts per million [ppm]) and radon (averaging 641 pCi/L [2.37 x 10^4 Bq/m^3]). The indoor-radon hazard potential is high where the alluvium occurs near Little Cottonwood Canyon. At the mouth of Provo Canyon in east Provo this alluvium contains detritus from uraniferous rocks of the Penn-

sylvanian to Mississipian Manning Canyon Shale and Precambrian Mineral Fork Formation, mixed with a significant fraction of material from less uraniferous rocks. Uranium (averaging 2.3 ppm) and radon (averaging 394 pCi/L [1.46 x 10^4 Bq/m^3] levels in this alluvium are lower in east Provo than in east Sandy, but are sufficiently high to indicate a moderate potential indoor-radon hazard where the alluvium occurs in east Provo.

Characterization of the uranium concentration, soil-gas radon level, and ground-water depth in geologic units underlying large areas can be accomplished rapidly, and can serve as a predictive indicator of the potential for high indoor-radon levels. This relative radon-hazard potential can then be used to prioritize indoor testing in existing buildings and evaluate the need for radon-resistant new construction.

INTRODUCTION

Concentrations of indoor radon (Rn) are a function of a number of non-geologic factors including weather, building construction, and ventilation. Ultimately, however, the source of the radon is uranium (U) in the geologic units surrounding a building's foundation. Identification of areas with high concentrations of uranium is the first step in determining the potential for high concentrations of indoor radon. One radon isotope, ^{222}Rn, is the most significant contributor to the indoor-radon problem and forms as a product in the ^{238}U decay series. Subsequent references to radon and uranium refer to these isotopes, unless otherwise noted.

The problem of radon in the domestic environment was first recognized in 1984 when a house in Boyertown, Pennsylvania was discovered to have indoor-radon concentrations of greater than 2,500 pCi/L (9.25 x 10^4 Bq/m^3). This occurrence is associated with Precambrian gneiss containing high levels of uranium. The radon levels in homes overlying this gneiss increase when it is sheared (Gundersen and others, 1988).

Sprinkel (1987) used regional geologic data to map potential radon-hazard areas in Utah. These areas were identified by known uranium occurrences; uranium-enriched rocks at the surface or beneath well-drained, porous, and permeable soils; and anomalous surficial uranium concentrations. The vicinity of the surface trace of the Wasatch fault zone, a large, permeable conduit in which uraniferous fluids and radon may readily migrate, was also considered a potential radon-hazard area. Quaternary units were not included in the compilation unless already documented as a radon source.

In 1988, in response to growing national concern over the threat of radon gas, Congress enacted Title III, Indoor Radon Abatement Act (IRAA), as an amendment to the Toxic Substances Control Act. The IRAA has the overall goal of reducing public health risks from radon gas by rendering air within buildings in the United States free of radon. Section 306 of the IRAA, the State Indoor Radon Grant (SIRG) Program, authorizes the U.S. Environmental Protection Agency (EPA) to provide grants to states to support development and implementation of state radon assessment and mitigation programs. A principal SIRG activity of the Utah Geological Survey (UGS) is to identify areas throughout the state that have geologic factors conducive to elevated indoor-radon levels, and assess the radon-hazard potential of those areas.

Indoor-radon levels were measured statewide during a 1988 survey conducted by the Utah Division of Radiation Control (UDRC) (Sprinkel and Solomon, 1990). Volunteers were solicited from cities or towns in radon-hazard areas defined by Sprinkel (1987); homes selected for testing were owner-occupied, single-family dwellings. Alpha-track detectors (ATDs) were placed in 631 homes to measure indoor-radon levels. The statewide average indoor-radon level was 2.7 picocuries per liter (pCi/L) (100 Becquerels per cubic meter [Bq/m^3]), with 14 percent of measurements greater than 4 pCi/L (148 Bq/m^3), the level above which hazard-reduction procedures are suggested (U.S. Environmental Protection Agency and others, 1992). Comparable figures for the United States are an average of 1.7 pCi/L (63 Bq/m^3) with 6 percent of measurements greater than 4 pCi/L (148 Bq/m^3) (Sextro, 1988). Clusters of high indoor-radon values occur in several areas of the state. Two of these areas, east Sandy and east Provo, occur along the populous Wasatch Front (figure 1) and were selected for detailed investigation during the first year of the multi-year SIRG program. This study included collection and interpretation of ground radiometric and geologic data in both areas, collection of additional indoor-radon measurements in homes and schools by the UDRC, and interpretation of airborne radiometric data in east Sandy and adjacent portions of the Salt Lake Valley and Wasatch Range. Preliminary results of this study were reported in Solomon and others (1991).

The objective of this investigation was to use rapid and inexpensive field methods to identify radon-hazard-potential areas based on geologic factors which influence areal radon distribution. These methods can be used elsewhere to assess the radon hazard prior to expenditure of considerable time and expense testing existing construction and using radon-resistant techniques in new construction.

LOCATION AND GEOLOGY OF STUDY AREAS

The east Sandy study area is in the Salt Lake Valley of eastern Salt Lake County. The study area extends from the mouth of Big Cottonwood Canyon on the north to the city of Draper on the south, and is approximately bounded by State Street on the west and the Wasatch Range on the east (figure 1). The average indoor-radon level in east Sandy is 3.0 pCi/L (111 Bq/m^3), with 18 percent of measurements greater than 4 pCi/L (148 Bq/m^3) (tables 1 and A-1).

The valley in Sandy is underlain by a complex sequence of Quaternary unconsolidated alluvial, colluvial, deltaic, lacustrine, eolian, and glacial deposits (figure 2) (Personius and Scott, 1992). The dominant influence on surficial geology and physiography was the last cycle of Pleistocene Lake Bonneville, which was present from about 28,000 to 13,000 years ago (Oviatt and others, 1992). The lake underwent several major periods of stability resulting in the creation of four basin-wide shorelines. Two of these, the transgressive Bonneville and regressive Provo shorelines, occur in the study area.

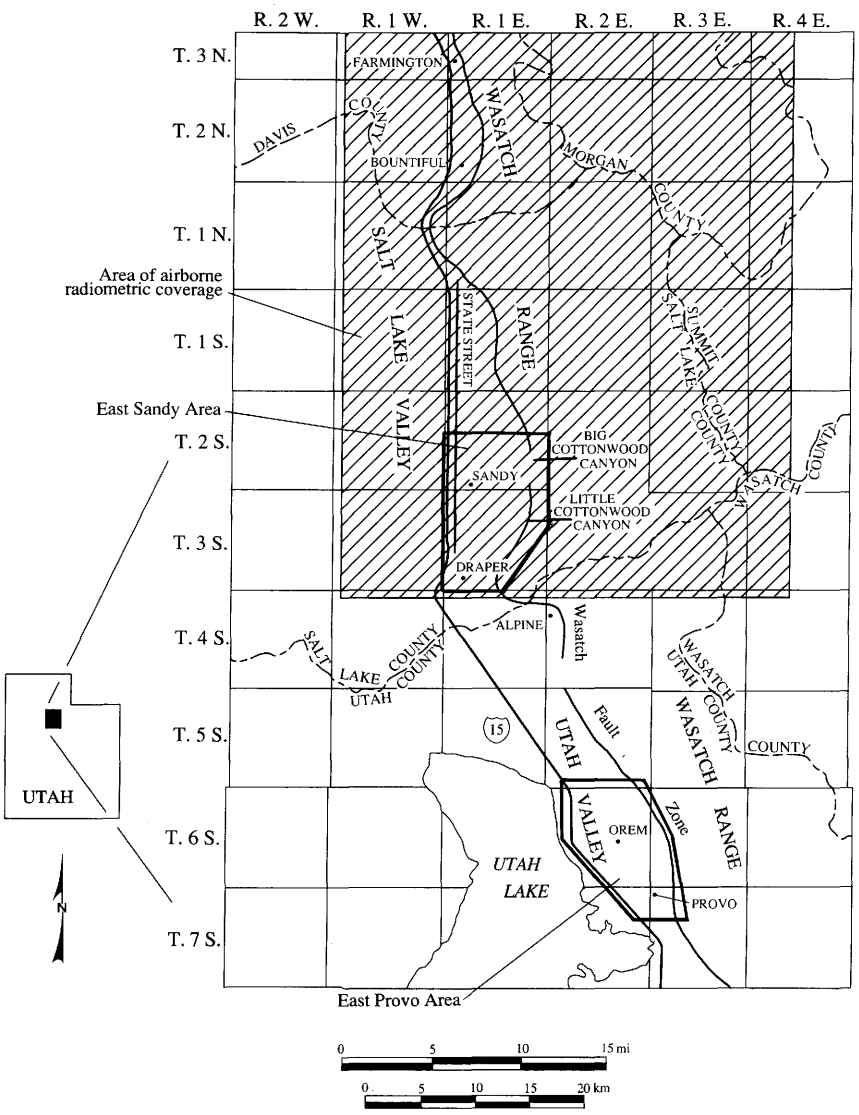

Figure 1. *Index map of study areas.*

Compound deltas at both the Bonneville and Provo levels were formed at the mouths of Big and Little Cottonwood Canyons by rivers which incised middle and upper Pleistocene glacial material and drained into the lake from the Wasatch Range. Uppermost Pleistocene and Holocene fluvial, alluvial-fan, colluvial, and eolian deposits overlie older, upper Pleistocene lacustrine and deltaic material. Coarser deposits in the valley generally occur to the east beneath elevated shoreline benches along the range front. Ground water is deeper than 50 feet (15 m) beneath the benches, but is less than 10 feet (3 m) deep beneath the valley floor to the west and beneath alluvial channels which dissect the benches (Anderson and others, 1986b). In Sandy, the active Wasatch fault zone separates unconsolidated deposits of the Salt Lake Valley from bedrock in the Wasatch Range.

A variety of bedrock crops out in the Wasatch Range, but three lithologies are potential sources of uranium for valley deposits. Of primary importance are Oligocene granitic rocks of the Little Cottonwood, Alta, and Clayton Peak stocks, which underlie extensive parts of the Little Cottonwood Canyon drainage and smaller parts of the Big Cottonwood Canyon drainage (Crittenden, 1976). Of secondary importance are informally named Precambrian metamorphic rocks and the Precambrian Mineral Fork Formation, a diamictite derived from older granitic rocks (Condie, 1967). These units underlie small parts of both canyon drainages. Quartzite, shale, and slate are widespread in the Precambrian Big Cottonwood Formation in the Big Cottonwood Canyon drainage (James, 1979), and provide source material low in uranium for valley deposits.

The east Provo study area is in the Utah Valley of central

Table 1.

Statistical summary of field data, factor ratings, hazard ratings, and hazard potential for Quaternary geologic units in the east Sandy area. Geologic units were mapped by Personius and Scott (1990, 1992) (figure 2), but units ca, alp, and lbg have been subdivided for this study where they occur on the Big Cottonwood and Little Cottonwood deltas. Soil textures are described using the classification of the U.S. Soil Conservation Service (1975) and reflect the predominant texture of the material at sample sites. Because of textural variability within geologic units, textures do not necessarily correspond to unit descriptions. N for eU and soil-gas Rn is the number of sample sites; N for ground-water depth is the number of sites with ground-water depth greater than 50 feet (15 m); N for indoor Rn is the number of sample sites for both this study and the statewide survey (Sprinkel and Solomon, 1990). Factor ratings for units with no samples collected were estimated from geologically similar units and indoor measurements. See tables 7 and 8 for a description of the factor ratings, hazard ratings, and hazard potential.

Geologic Unit	Soil Texture	eU					Rn in soil gas					Depth to ground water			Indoor Rn				Hazard Rating and Potential
		N	%>3 ppm	Avg. ppm	Max. ppm	Rating	N	%>500 pCi/L	Avg. pCi/L	Max. pCi/L	Rating	N	%>50 ft	Rating	N	%>4 pCi/L	Avg. pCi/L	Max. pCi/L	
Lacustrine Deposits																			
Deposits postdating the Bonneville lake cycle																			
Lacustrine, marsh, and alluvial deposits (laly)	CL	2	50	3.2	3.3	2	2	50	522	905	3	0	0	1	0	–	–	–	6 - Mod
Regressive-phase deposits of Bonneville lake cycle																			
Deltaic deposits (lpd)	Sg	7	86	7.1	9.0	4	3	33	315	613	2	1	11	1	2	0	1.1	1.3	7 - Mod
Lacustrine gravel (lpg)	Sg	33	76	4.8	10.6	3	19	47	539	1,434	3	44	59	3	42	7	2.2	8.8	9 - Mod
Transgressive-phase deposits of Bonneville lake cycle																			
Lacustrine gravel (lbg)	Sg	17	82	4.8	8.6	–	8	38	565	1,198	–	26	74	–	18	22	3.5	26.2	–
Big Cottonwood	Sg	2	100	7.1	8.6	4	2	0	296	327	2	0	0	1	2	0	0.8	1.1	7 - Mod
Little Cottonwood	Sg	15	80	4.5	7.9	3	6	50	654	1,198	3	26	84	4	16	25	3.8	26.2	10 - Hi
Undivided deposits of Bonneville lake cycle																			
Lacustrine clay and silt (lbpm)	CL	2	50	3.8	5.1	2	2	50	445	580	2	0	0	1	1	0	0.8	0.8	5 - Low
Alluvial Deposits																			
Stream alluvium																			
Unit 1 (al1)	Sg	6	83	6.8	9.0	3	3	0	270	482	2	0	0	1	1	0	1.1	1.1	6 - Mod
Unit 2 (al2)	Slg	1	100	3.7	3.7	2	0	–	–	–	4	0	0	1	5	80	9.0	26.2	7 - Mod
Regressive-phase alluvium (alp)	LSg	34	97	6.7	8.7	–	16	50	641	2,398	–	78	64	–	88	27	3.7	13.7	–
Big Cottonwood	LSg	2	50	4.1	5.5	2	0	–	–	–	3	0	0	1	4	0	2.5	3.8	6 - Mod
Little Cottonwood	LSg	32	100	6.9	8.7	4	16	50	641	2,398	3	78	67	3	84	29	3.8	13.7	10 - Hi

***Table 1** (continued)*

Fan alluvium																			
Unit 1 (af1)	Sg	1	100	4.2	4.2	2	0	–	–	–	1	1	100	4	0	–	–	–	7 - Mod
Unit 2 (af2)	Sg	6	67	4.0	6.0	2	1	0	120	120	1	6	55	3	5	0	2.5	3.2	6 - Mod
Glacial Deposits																			
Outwash of Bells Canyon age (gbco)	Sg	2	100	7.0	7.4	4	0	–	–	–	3	3	100	4	1	0	2.7	2.7	11 - Hi
Till of Bells Canyon age (gbct)	Sg	2	100	5.7	6.3	3	0	–	–	–	3	3	100	4	1	100	6.1	6.1	10 - Hi
Eolian Deposits																			
Sand (es)	S	8	88	5.1	8.2	3	0	–	–	–	2	30	83	4	28	0	1.7	3.4	9 - Mod
Colluvial Deposits																			
Debris-flow deposits 1 (cd1)	Sg	0	–	–	–	3	0	–	–	–	2	2	100	4	2	0	1.6	1.9	9 - Mod
Hillslope colluvium (chs)	Sg	2	100	5.7	5.7	3	0	–	–	–	3	3	100	4	1	0	2.4	2.4	10 - Hi
Colluvium and alluvium (ca)	Sg	8	100	5.9	8.4	–	2	0	375	467	–	12	67	–	10	10	2.1	4.4	–
Big Cottonwood	Sg	4	100	5.5	8.4	3	2	0	375	467	2	1	20	1	1	0	2.2	2.2	6 - Mod
Little Cottonwood	Sg	4	100	6.4	7.7	3	0	–	–	–	3	11	85	4	9	11	2.1	4.4	10 - Hi
Fill Deposits																			
Man-made fill (f)	Sg	0	–	–	–	4	0	–	–	–	3	1	100	4	1	0	2.2	2.2	11 - Hi
EAST SANDY TOTAL	–	131	86	5.6	10.6	–	56	41	528	2,398	–	210	62	–	206	18	3.0	26.2	–

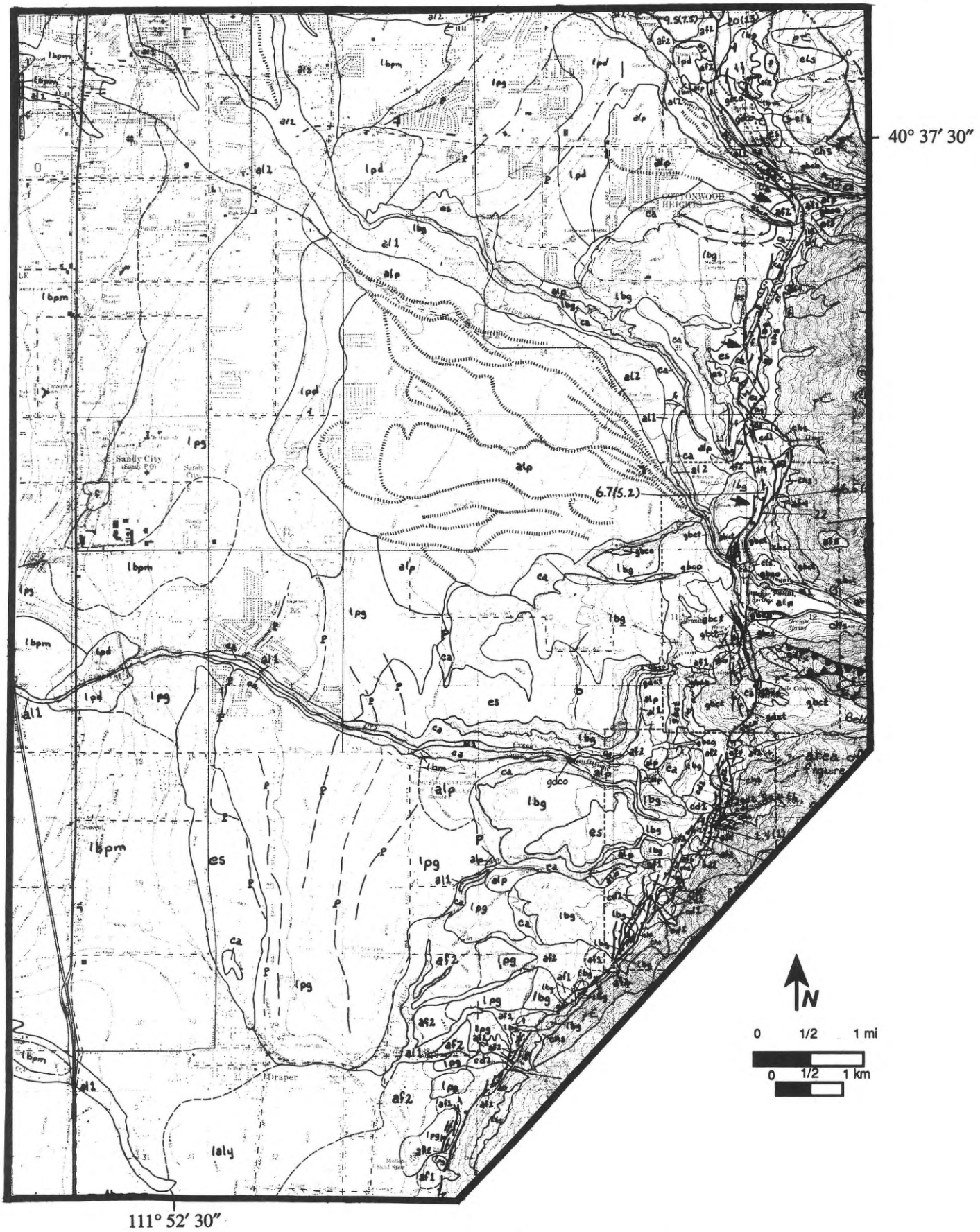

Figure 2. *Surficial geologic map of the east Sandy study area, modified from Personius and Scott (1990).*

***Figure 2** (continued)*

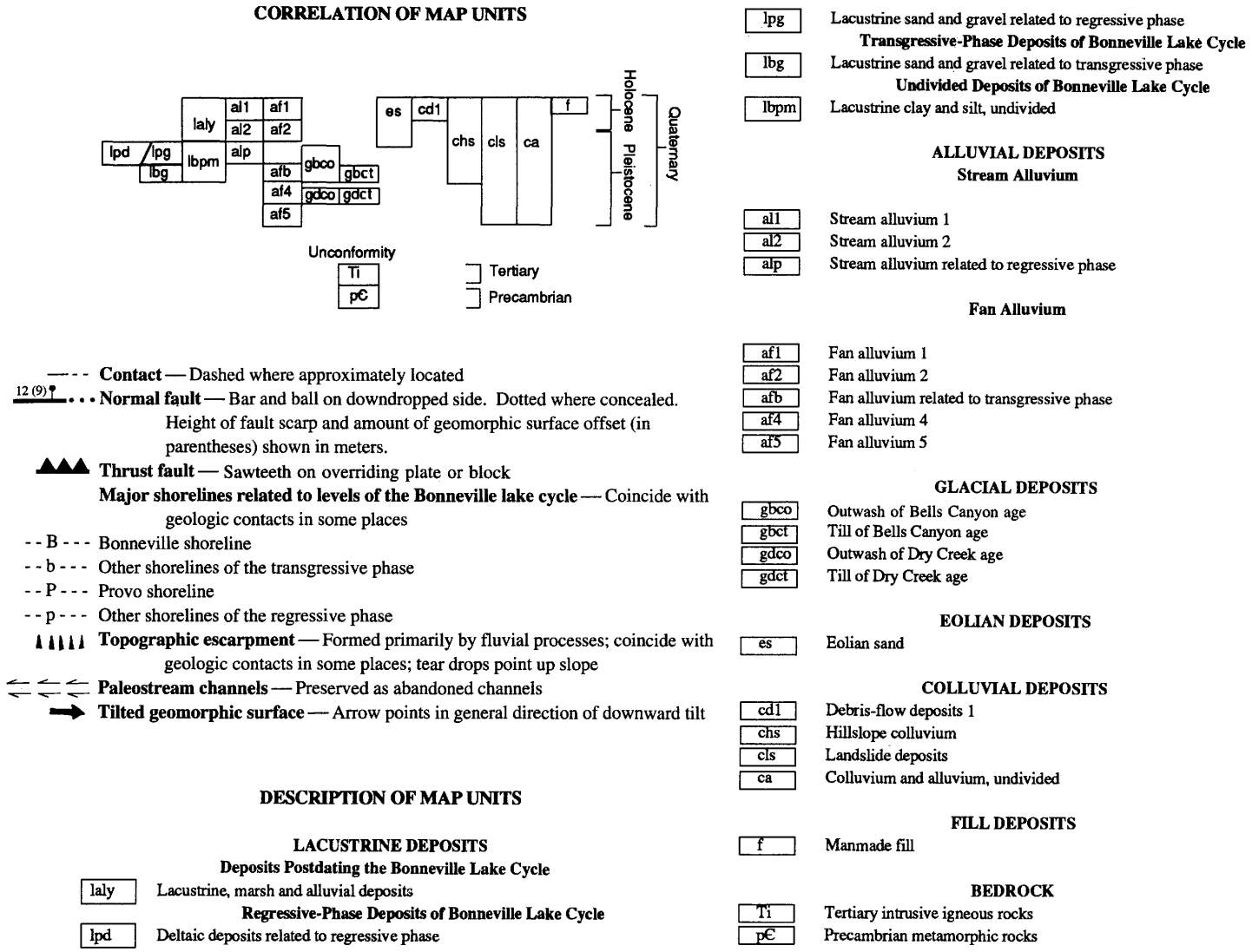

Utah County. The study area extends from the city of Orem on the north to Provo on the south, and is approximately bounded by Interstate 15 on the west and the Wasatch Range on the east (figure 1). The average indoor-radon level in east Provo is 2.5 pCi/L (93 Bq/m^3), with 12 percent of measurements greater than 4 pCi/L (148 Bq/m^3) (tables 2 and A-2). Although the average indoor-radon level in the study area is lower than the statewide average, Sprinkel and Solomon (1990) demonstrated that part of east Provo has average indoor-radon concentrations in excess of the statewide average.

The valley in Provo is underlain by Quaternary sediments deposited in similar paleoenvironments to those of east Sandy (figure 3) (Machette, 1989). A compound delta at both the Bonneville and Provo levels was formed at the mouth of Provo Canyon by a river which drained into Lake Bonneville from the Wasatch Range. Ground water is deeper than 50 feet (15 m) in coarser deposits underlying elevated shoreline benches along the range front, but is less than 10 feet (3 m) deep beneath the valley floor to the west and beneath alluvial channels which dissect the benches (Anderson and others, 1986a). As in Sandy, the Wasatch fault zone separates unconsolidated deposits of the valley from bedrock in the mountains.

A variety of bedrock crops out in the Wasatch Range adjacent to the east Provo area. Two units are potential sources of uranium for valley deposits: (1) the Pennsylvanian to Mississippian Manning Canyon Shale, a dark, organic shale which underlies a large portion of the range front; and (2) diamictite of the Precambrian Mineral Fork Formation, similar to that near Sandy, which underlies the Rock and Slate Canyon drainages (Baker, 1964, 1972, 1973). Limestone and quartzite of the Pennsylvanian and Permian Oquirrh Formation provide source material low in uranium for valley deposits, and underlie much of the Provo Canyon drainage.

Table 2.

Statistical summary of field data, factor ratings, hazard ratings, and hazard potential for Quaternary geologic units in the east Provo area. Geologic units were mapped by Machette (1989) (figure 3). Soil textures are described using the classification of the U.S. Soil Conservation Service (1975) and reflect the predominant texture of the material at sample sites. Because of textural variability within geologic units, textures do not necessarily correspond to unit descriptions. N for eU and soil-gas Rn is the number of sample sites; N for ground-water depth is the number of sites with ground-water depth greater than 50 feet (15 m); N for indoor Rn is the number of sample sites for both this study and the statewide survey (Sprinkel and Solomon, 1990). Factor ratings for units with no samples collected were estimated from geologically similar units and indoor measurements. See tables 7 and 8 for a description of the rating factors and hazard ratings.

Geologic Unit	Soil Texture	eU					Rn in soil gas					Depth to ground water			Indoor Rn				Hazard Rating and Potential
		N	%>3 ppm	Avg. ppm	Max. ppm	Rating	N	%>500 pCi/L	Avg. pCi/L	Max. pCi/L	Rating	N	%>50 ft	Rating	N	%>4 pCi/L	Avg. pCi/L	Max. pCi/L	
Lacustrine Deposits																			
Regressive-phase deposits of Bonneville lake cycle																			
Deltaic deposits (lpd)	Lg	2	0	2.1	2.2	2	2	0	190	205	1	0	0	1	5	0	1.7	2.3	4 - Low
Lacustrine gravel (lpg)	Lg	3	0	1.9	2.4	1	2	0	384	419	2	0	0	1	8	0	1.9	2.5	4 - Low
Lacustrine sand (lps)	CLg	4	0	2.3	2.9	2	4	50	421	619	2	0	0	1	3	0	1.4	1.7	5 - Low
Lacustrine silt and clay (lpm)	CL	0	–	–	–	1	0	–	–	–	1	0	0	1	5	0	1.2	1.9	3 - Low
Transgressive-phase deposits of Bonneville lake cycle																			
Lacustrine gravel (lbg)	Lg	2	50	3.1	3.8	2	0	–	–	–	3	6	100	4	4	0	2.8	3.7	9 - Mod
Lacustrine sand (lbs)	Lg	9	44	2.7	3.4	2	3	0	154	207	1	25	96	4	17	6	1.8	9.9	7 - Mod
Lacustrine silt and clay (lbm)	Lg	10	50	2.9	3.6	2	7	57	602	1,463	3	18	51	3	24	25	3.7	13.6	8 - Mod
Alluvial Deposits																			
Stream alluvium																			
Unit 1 (al1)	SLg	2	50	3.0	4.0	2	1	0	187	187	1	0	0	1	0	–	–	–	7 - Mod
Unit 2 (al2)	SLg	8	13	2.4	3.9	2	3	67	604	887	3	0	0	1	2	50	3.8	6.5	6 - Mod
Regressive-phase alluvium (alp)	Lg	24	17	2.3	3.3	2	11	27	394	734	2	21	38	2	31	6	2.5	6.3	6 - Mod

***Table 2** (continued)*

Fan alluvium																			
Unit 2 (af2)	Lg	8	25	2.5	3.4	2	6	33	679	1,455	3	0	0	1	1	100	8.2	8.2	6 - Mod
Younger fan alluvium (afy)	Lg	19	32	2.9	4.6	2	11	45	517	1,405	3	26	49	2	34	18	2.7	10.2	7 - Mod
Regressive-phase fan alluvium (afp)	Lg	6	33	2.8	3.6	2	5	0	234	468	1	1	6	1	10	10	1.9	8.1	4 - Low
Transgressive-phase fan alluvium (afb)	Lg	0	–	–	–	1	0	–	–	–	3	1	100	4	1	0	1.4	1.4	8 - Mod
Unit 4 (af4)	Lg	0	–	–	–	1	0	–	–	–	3	1	100	4	1	0	0.9	0.9	8 - Mod
Eolian Deposits																			
Sand and silt (es)	SCL	2	0	1.8	1.8	1	2	0	419	490	2	0	0	1	5	0	2.0	3.8	4 - Low
Colluvial Deposits																			
Older landslide deposits (clso)	Lg	0	–	–	–	2	0	–	–	–	3	1	100	4	1	0	3.4	3.4	9 - Mod
EAST PROVO TOTAL	–	99	26	2.6	4.6	–	57	32	449	1,463	–	100	40	–	152	12	2.5	13.6	–

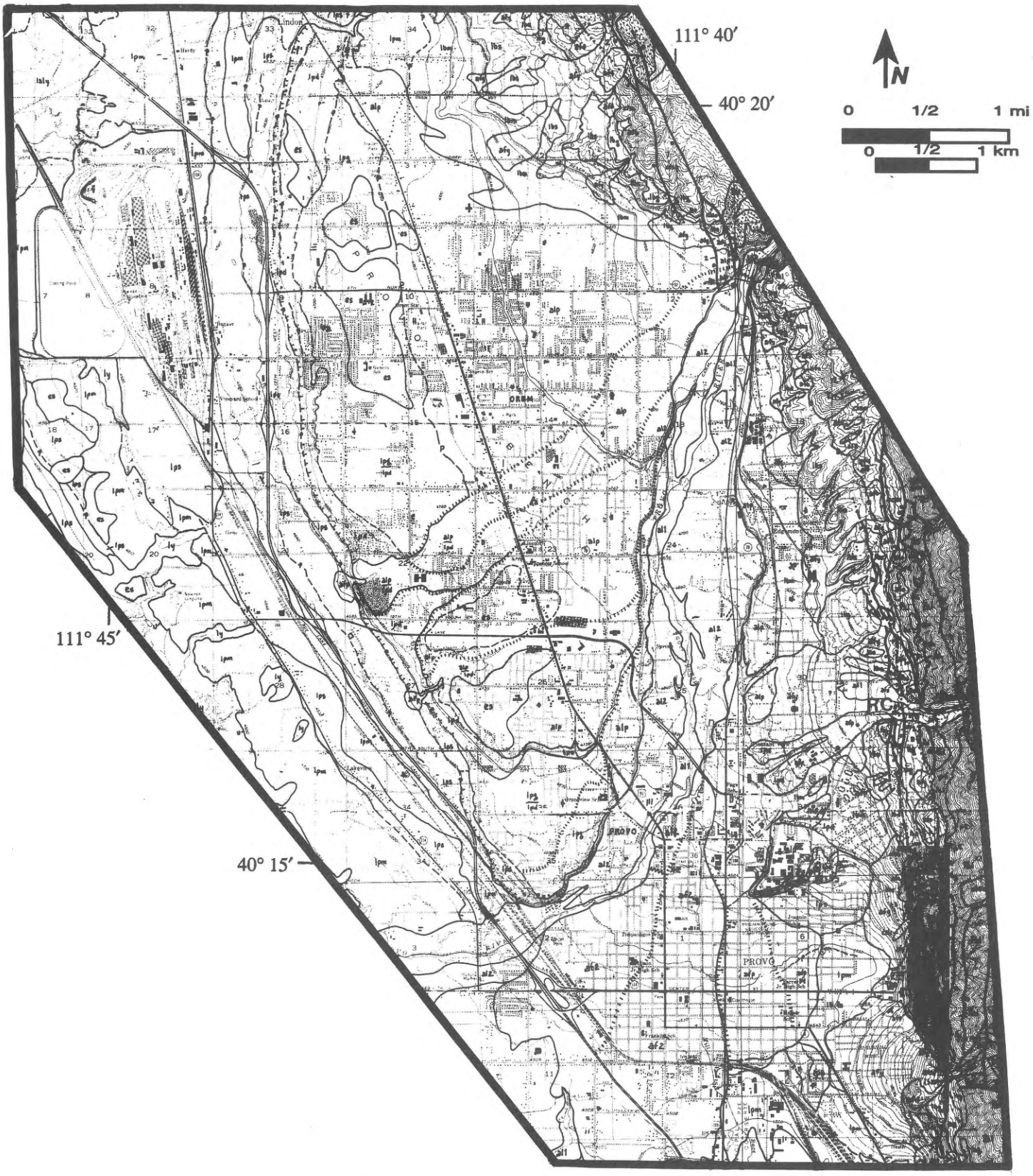

Figure 3. *Surficial geologic map of the east Provo study area, modified from Machette (1989).*

***Figure 3** (continued)*

CORRELATION OF MAP UNITS

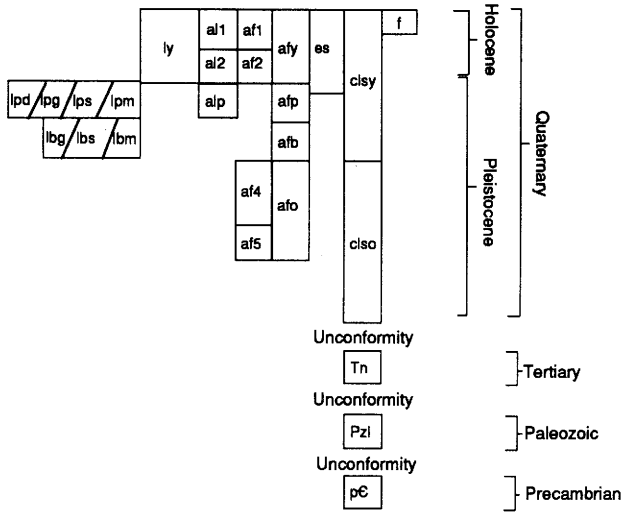

Contact — Dashed where approximately located

Gradational contact — Contact between differentiated units and undifferentiated counterparts.

12 (9) / RC **Normal fault** — Bar and ball on downdropped side. Dotted where concealed. Height of fault scarp and amount of geomorphic surface offset (in parentheses) shown in meters. RC shows location of exploratory trench

Major shorelines related to levels of the Bonneville lake cycle — Coincide with geologic contacts in some places

- - B - - - Bonneville shoreline
- - P - - - Provo shoreline
- - p - - - Other shorelines of the regressive phase

Topographic escarpment — Formed primarily by fluvial processes; coincide with geologic contacts in some places; where escarpment coincides with the contact between map units, hachures face up slope

Tilted geomorphic surface — Arrow points in general direction of downward tilt

DESCRIPTION OF MAP UNITS

LACUSTRINE DEPOSITS

Deposits Postdating the Bonneville Lake Cycle

ly	Younger lacustrine and marsh deposits

Regressive-Phase Deposits of Bonneville Lake Cycle

lpd	Deltaic deposits related to regressive phase
lpg	Lacustrine gravel related to regressive phase
lps	Lacustrine sand related to regressive phase
lpm	Lacustrine silt and clay related to regressive phase

Transgressive-Phase Deposits of Bonneville Lake Cycle

lbg	Lacustrine gravel related to transgressive phase
lbs	Lacustrine sand related to transgressive phase
lbm	Lacustrine silt and clay related to transgressive phase

ALLUVIAL DEPOSITS

Stream Alluvium

al1	Stream alluvium 1
al2	Stream alluvium 2
alp	Stream alluvium related to regressive phase

Fan Alluvium

af1	Fan alluvium 1
af2	Fan alluvium 2
afy	Younger fan alluvium, undivided
afp	Fan alluvium related to regressive phase
afb	Fan alluvium related to transgressive phase
af4	Fan alluvium 4
af5	Fan alluvium 5
afo	Older fan alluvium, undivided

EOLIAN DEPOSITS

es	Eolian sand and silt

COLLUVIAL DEPOSITS

clsy	Younger landslide deposits
clso	Older landslide deposits

FILL DEPOSITS

f	Manmade fill

BEDROCK

Tn	Neogene sedimentary rocks
Pzl	Paleozoic sedimentary rocks, lower part
pЄ	Proterozoic and Archean rocks

DATA COLLECTION AND INTERPRETATION

The hazard from indoor radon is difficult to assess due to the influence of building construction quality and techniques and occupant lifestyle; effective indoor monitoring requires testing every home. However, airborne-radiometric data exist over most of the U.S. and are useful for identifying areas with the potential for an indoor-radon hazard. Muessig (1988) compared airborne radiometrics collected for the National Uranium Resource Evaluation (NURE) with indoor radon in New Jersey, and found that areas with mean equivalent uranium (eU) concentrations greater than 2.4 ppm are associated with radon levels in homes greater than 4 pCi/L (148 Bq/m^3). Identification of uranium anomalies using airborne-radiometric data allows follow-up ground surveys in relatively small areas. The surveys include assessment of pertinent geologic factors and measurement of radon in homes. Acquisition of more detailed information may result in building code requirements to reduce the susceptibility of homes to radon.

Airborne-Radiometric Measurements

Sampling and Analytical Techniques

The airborne-radiometric survey completed under the NURE program permits delineation of areas of high surface-uranium concentrations that indicate potential for an indoor-radon hazard (Duval and Otton, 1990). Geologic units responsible for the hazard typically are widespread and may affect homes in a large area. NURE data were collected on a coarse scale, generally with 5-kilometer (3-mi) line spacings and 10-kilometer (6-mi) spacings on tie lines. The data, therefore, serve as a reconnaissance tool for regional studies, but more detailed follow-up surveys such as ground-based gamma-ray spectrometry, soil-radon emanometry, and indoor-radon measurements are required to accurately characterize the hazard. Radon hazards resulting from small point sources, such as uranium-mill tailings used for foundation soils, cannot be detected using NURE data.

NURE data (EG&G Geometrics, 1979) were compiled for the eastern Salt Lake Valley and adjacent parts of the Wasatch Range (figure 1). The airborne survey was performed using a helicopter-mounted GeoMetrics GR-800 gamma-ray spectrometer. The GR-800 system contained 37,760 cubic centimeters (2,304 in^3) of NaI crystals. Navigation of the helicopter was with visual techniques and 1:24,000 topographic maps, but the flight paths were also documented using a 35-mm tracking camera. The survey was flown at a terrain clearance of between 60 and 210 meters (200 and 700 ft), with an average clearance of 120 meters (400 ft). Data were collected at 1-second intervals along the flight lines. Data-reduction techniques are described in the NURE report (EG&G Geometrics, 1979).

Data and Discussion

Corrected NURE values for eU, equivalent thorium-232 (eTh), and potassium-40 (K) were used to plot eU, eTh, and K concentration, total gamma, and eU/eTh, eU/K, and eTh/K contour maps (figures 4 through 10). The contour maps were generated by computer and have no geologic bias. The eU and total-gamma contour maps are useful for delineating areas that require ground survey follow-up. The eTh contour map is useful because ^{232}Th decays to ^{220}Rn and, although the half-life of this isotope is much shorter than that of ^{222}Rn, ^{220}Rn may be a significant contributor to the indoor-radon hazard in buildings built on Th-rich ground (Stranden, 1984). The ratio maps, commonly used in uranium exploration to define areas having the potential for ore deposits, are used here with the eU, eTh, and K contour maps to determine the nature of the source rock from which Rn-generating sediments were derived.

The average apparent uranium concentration for the Salt Lake City 1:250,000-scale quadrangle is 1.65 ppm (EG&G Geometrics, 1979). The area of interest for this study is uranium anomaly A in Sandy (figure 4). Uranium concentrations are greater than 3.2 ppm in the area where high levels of indoor radon were detected in the 1988 UDRC survey (Sprinkel and Solomon, 1990). The anomaly corresponds to locally derived Quaternary unconsolidated deposits along the front of the Wasatch Range. The high uranium values in the Wasatch Range east of anomaly A (figure 4) are located over the Little Cotton-

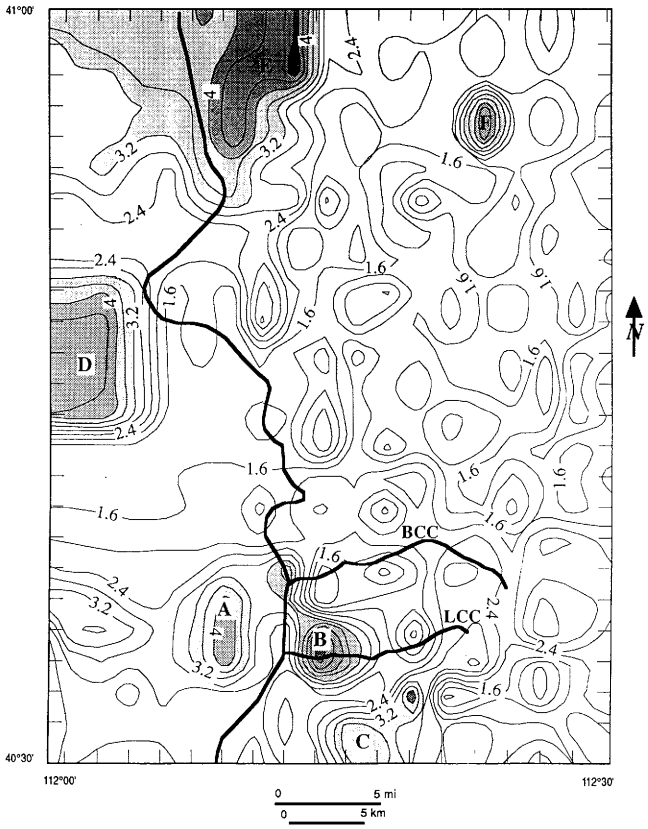

Figure 4. Equivalent uranium concentrations from the airborne-radiometric survey. The heavy line is the range front. BCC is Big Cottonwood Canyon; LCC is Little Cottonwood Canyon. Anomalies A through F are discussed in the text. Contour interval 0.4 ppm. Anomalies with concentrations greater than 4.0 ppm have light shading between 3.2 and 4.0 ppm, moderate shading between 4.0 and 4.8 ppm, and dark shading greater than 4.8 ppm.

wood, Alta, and Clayton Peak stocks (anomaly B). This suggests that a significant portion of anomaly A results from granitic material eroded from the stocks.

Uranium anomaly A is coincident with a broader thorium anomaly that reaches values greater than 13 ppm (figure 5), and uranium anomaly B is coincident with even higher values of thorium over the granitic stocks. Diffuse patterns of elevated potassium concentrations (figure 6) are also associated with the uranium and thorium anomalies. The data are compatible with the process of concentration of U, Th, and K in more siliceous igneous rocks during the later stages of igneous-melt differentiation (Nielson and others, 1991).

The total-gamma count represents gamma radiation in the entire 0.4 to 3.0 million electron volts (MeV) range (figure 7). The total-gamma anomalies are much broader than the eU anomalies and thus less useful than the eU data for delineating areas requiring ground surveys.

There are no eU/eTh (figure 8), eU/K (figure 9), or eTh/K anomalies (figure 10) coincident with uranium anomaly A. This is expected given the high concentrations of uranium, thorium, and potassium in the area. If the uranium resulted from non-igneous processes, it would be concentrated relative to both Th and K and the ratio maps would be more useful.

Because high indoor-radon values are associated with uranium anomaly A, other areas with similarly high eU concentrations should be field checked. Anomaly C (figure 4) has such concentrations and is also coincident with an eTh anomaly (figure 5). Anomaly C is in an uninhabited area over different parts of the granitic stocks that produced anomaly B; however, drainage is to the south toward the town of Alpine in northern Utah Valley. Thus, a potential for high eU and related indoor-radon concentrations exists in the Alpine area.

Anomaly D (figure 4), elongated to the west due to a boundary effect of the contouring program, is over Lake Bonneville clays in northern Salt Lake Valley. The eU anomaly is not coincident with an eTh anomaly as in the Sandy area. No additional verification work has been done on this anomaly.

Anomaly E is over exposures of the Precambrian Farmington Canyon Complex, a unit with an average airborne eU concentration of 3.27 ppm (EG&G Geometrics, 1979), and extends westward over gravel derived from the unit (figure 4). An eTh anomaly is coincident with uranium anomaly E but, whereas the greatest uranium concentrations are in the Farmington Canyon Complex, the greatest eTh concentrations are in the gravel (figure 5). Thorium concentrations up to 22 ppm in anomaly E are the highest seen in this study. Although the Farmington Canyon Complex principally underlies uninhabited areas in the Wasatch Range, the gravel was deposited at the base of the range and could serve as a radon source in Wasatch Front communities from Farmington to Bountiful.

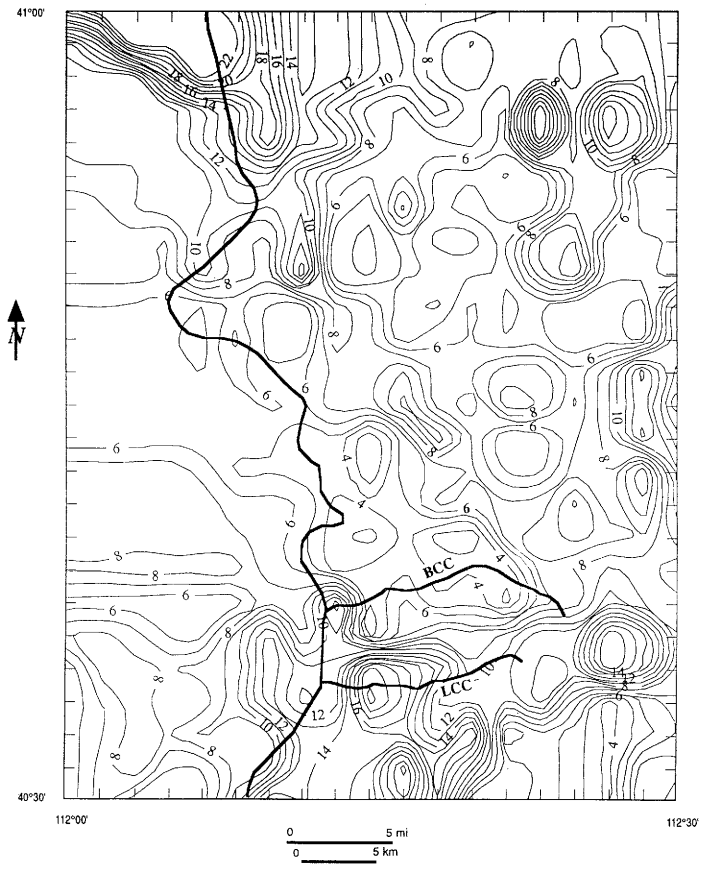

Figure 5. *Equivalent thorium concentrations from the airborne-radiometric survey. See figure 4 for explanation of symbols. Contour interval 1.0 ppm.*

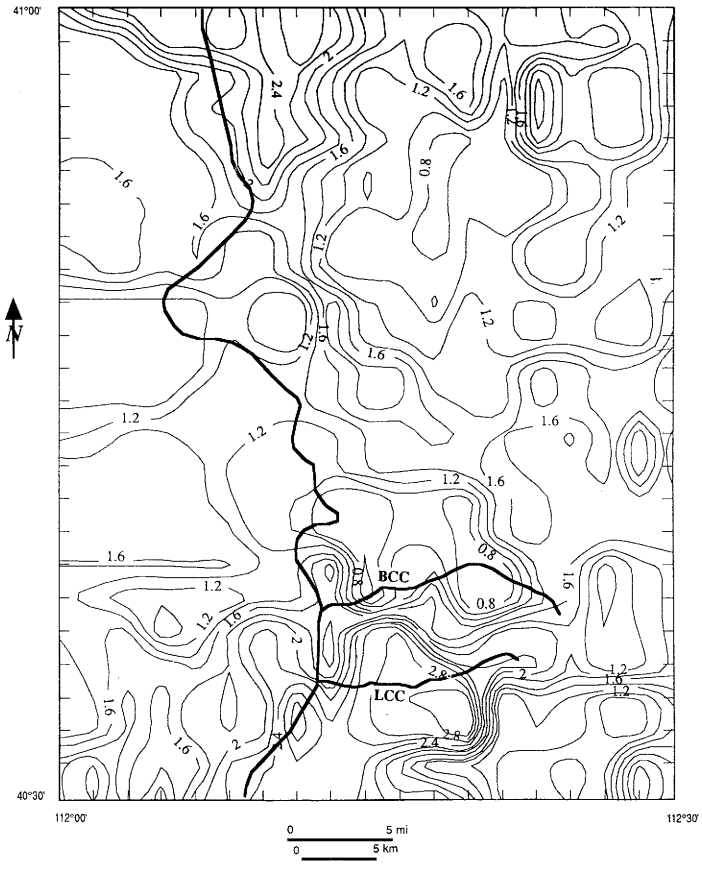

Figure 6. *Potassium concentrations from the airborne-radiometric survey. See figure 4 for explanation of symbols. Contour interval 0.2 percent.*

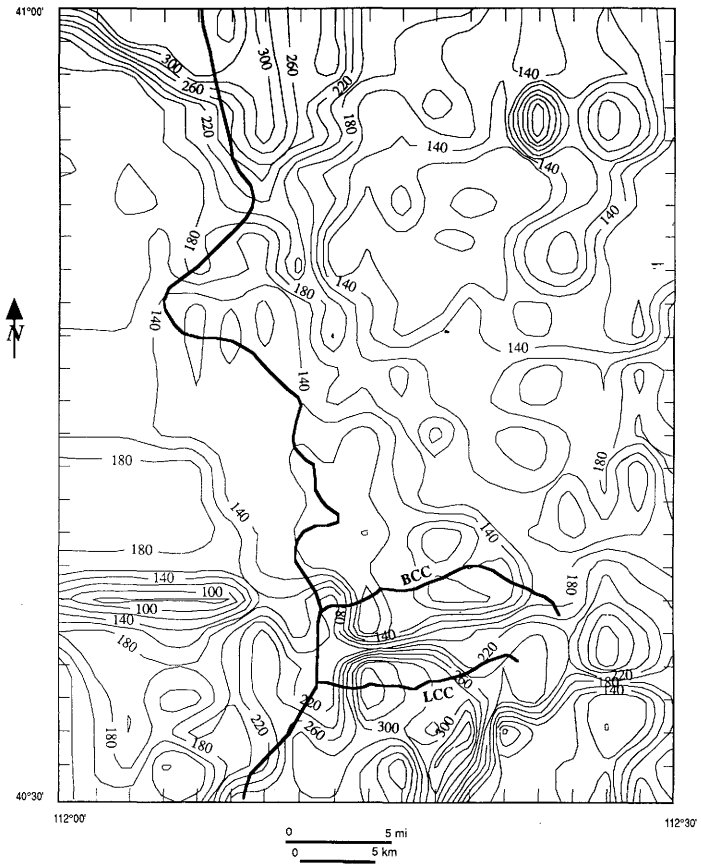

Figure 7. Total gamma count from the airborne-radiometric survey. See figure 4 for explanation of symbols. Contour interval 20 counts per second.

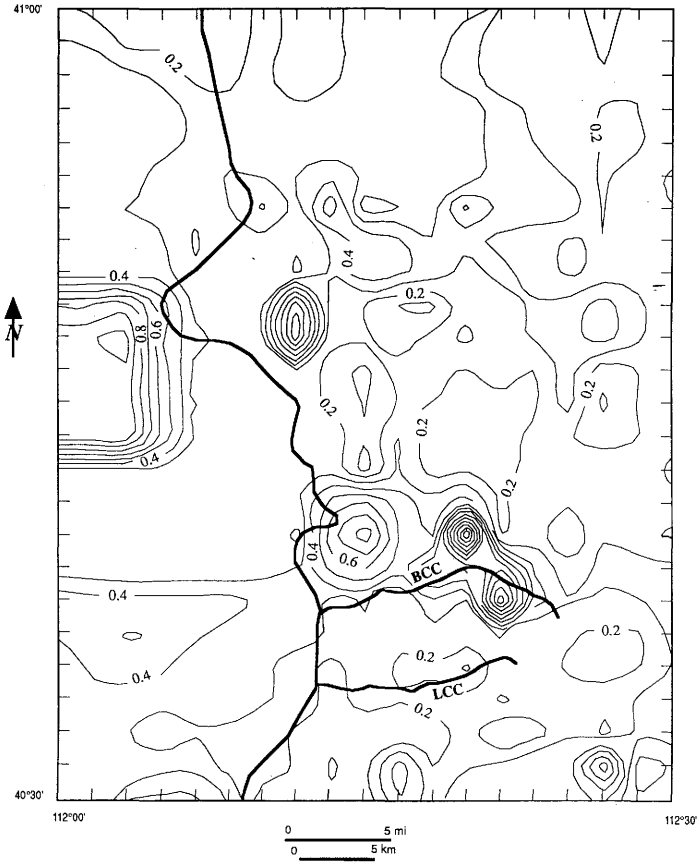

Figure 8. eU/eTh ratios from the airborne-radiometric survey. See figure 4 for explanation of symbols. Contour interval 0.1.

Anomaly F is over exposures of the Eocene Wasatch Formation (figure 4) and is also coincident with an eTh anomaly (figure 5). However, anomaly F is in an uninhabited area of southwestern Morgan County and poses little risk of a radon hazard.

Ground Measurements

Sampling and Analytical Techniques

Five types of ground data were collected during this study: (1) gamma-ray spectrometry, (2) soil-gas radon emanometry, (3) soil moisture and density, (4) soil texture, and (5) indoor-radon measurements in homes and schools. Gamma-ray spectrometry measures the amount of radioactive parent material in the soil available to decay to radon. Radon emanometry measures the level of radon in soil gas available for migration into buildings. Soil moisture, density, and texture affect the ability of radon to migrate through the soil to building foundations. Soil data were collected at 131 sites in the east Sandy area and 99 sites in the east Provo area. Indoor-radon measurements were made at 153 homes and 12 schools in the east Sandy area, and 66 homes and 4 schools in the east Provo area. These indoor measurements are from targeted surveys, and are in addition to those collected during the 1988 statewide survey (Sprinkel and Solomon, 1990). The results of 53 indoor measurements in the east Sandy area and 86 in the east Provo area from the statewide survey are included in statistical analyses in this report, and are summarized in Solomon and others (1991).

Concentrations of gamma-emitting elements in soil were measured using an Exploranium GR-256 portable, gamma-ray spectrometer with a GPS-21 detector. The detector contained a 3 x 3 inch (7.5 x 7.5 cm) NaI crystal. Values for total gamma, K, eU, and eTh were measured. Peak energy levels used for measurement were 1.46 MeV for K (K has only one emission line), 1.76 MeV for eU (corresponding to ^{214}Bi), and 2.62 MeV for eTh (corresponding to ^{208}Tl).

Two techniques were used to measure radon concentrations in soil gas. The first used an RDA-200 portable, alpha-sensitive scintillometer manufactured by EDA Instruments. Scintillator cells are coated with a phosphor sensitive to alpha particles (resulting from the decay of ^{222}Rn) in the 5.5 MeV range. Individual scintillator cells were calibrated using the UNC Geotech Alpha-track Chamber in Grand Junction, Colorado. The soil-gas sampling system consisted of a 0.4-inch (1-cm) diameter, hollow steel probe that was placed in a hole made by pounding into the soil a rod of slightly smaller diameter than the probe. The probe was inserted to a depth of 26 inches (65

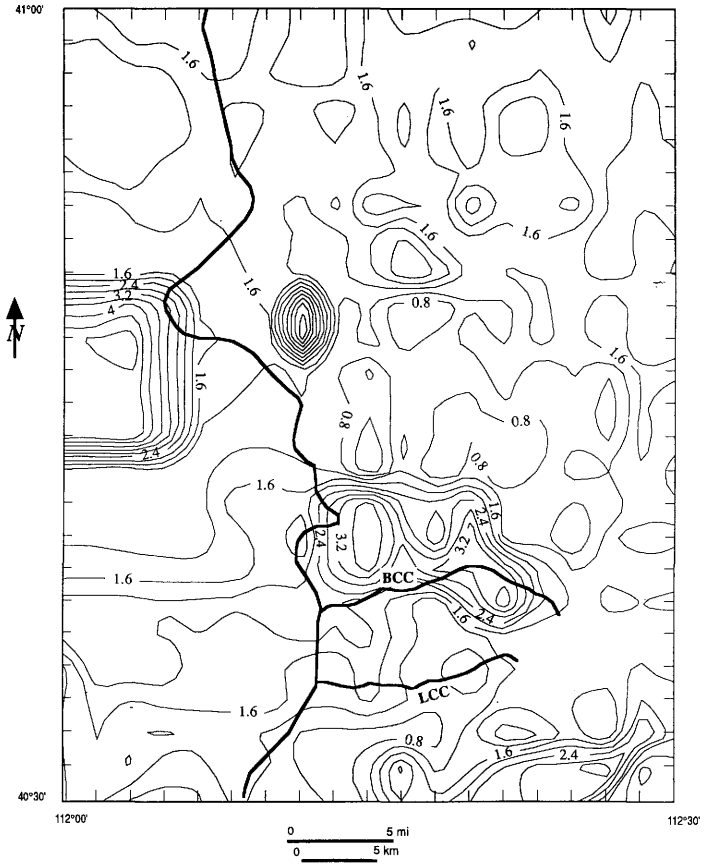

Figure 9. *eU/K ratios from the airborne-radiometric survey. See figure 4 for explanation of symbols. Contour interval 0.4.*

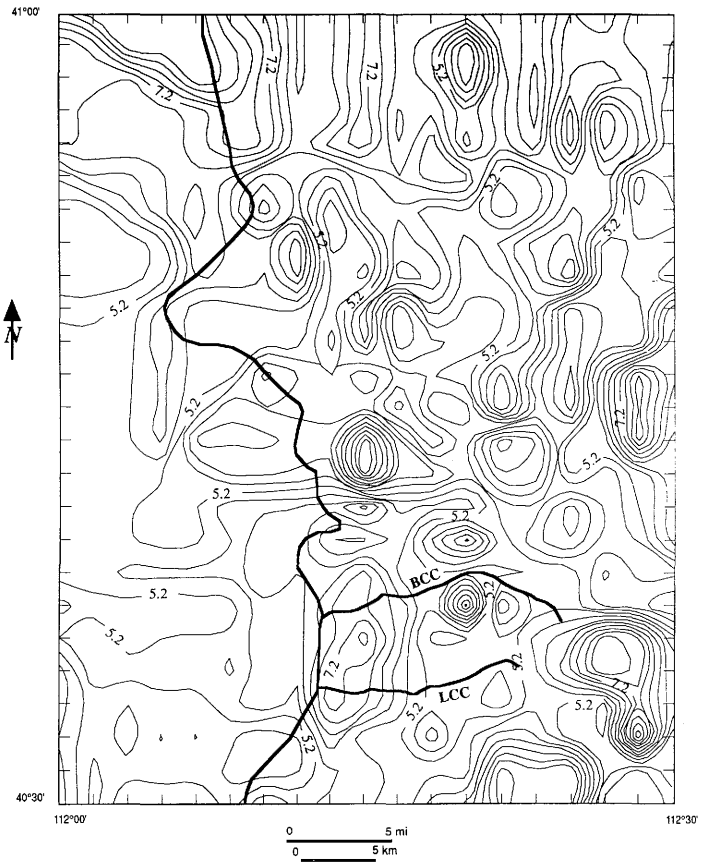

Figure 10. *eTh/K ratios from the airborne-radiometric survey. See figure 4 for explanation of symbols. Contour interval 0.4.*

cm), and samples were collected from perforations in the lower 6 inches (15 cm) of the probe. This depth allowed sample collection below the root zone for grasses, is within the lower B or upper C horizons of most soils, and is about the same as sampling depths which provided consistent and reproducible data to other researchers (Hesselbom, 1985; Reimer and Gundersen, 1989).

Initial scintillometer soil-gas measurements in the east Sandy area identified a pattern of high concentrations up to 2,398 pCi/L (8.87 x 10^4 Bq/m^3). This pattern was confirmed with a second technique using alpha-track detectors (ATDs) manufactured by Alpha Spectra, Inc. ATDs integrate the flux of radon gas over time, and thus average out short-term fluctuations produced by atmospheric variables. The Alpha Spectra units are designed for indoor use and quickly become saturated at higher exposure levels typically found in soil gas. They were therefore left in the ground for only 2 to 3 days. Several ATD surveys were made to evaluate the reproducibility of results, which were standardized for variations in atmospheric conditions during repetitive measurements at several sites.

The flux of radon from soil to the atmosphere can be defined by a diffusion model that depends on depth of source material (Tanner, 1964; Schery and others, 1984). Therefore, the depth at which the measurement is taken is important and, under ideal conditions, all soil-gas samples would be collected at the same depth. However, in the Sandy area, extremely variable soil conditions prohibited maintaining a constant sampling depth and measured values of soil-gas radon must be corrected for depth below the surface. Witcher and Schoenmackers (1990) have derived a relationship for correcting the measured radon concentration to the concentration at an infinite depth. This relationship is given by:

$$C_D = C_Z/(1-\exp[-(Øy_m/D)^{1/2}Z])$$

where:

C_D is the depth-corrected value

C_Z is the concentration at depth Z

y_m is the radon-decay constant (2.1 x 10^{-6})

Ø is porosity (0.35)

D is the bulk diffusion coefficient (0.01 cm^2/s [1.6 x 10^{-3} in^2/s]).

ATD data for the Sandy area were corrected using the above equation and constants.

Laboratory measurement of radon from soil samples was also made to determine radon provenance. About 100 grams (3.5 oz) of soil were collected from some sites tested in the field with ATDs. The samples were placed in jars, with an ATD taped to the inside of the lid when the jars were sealed. The ATDs were exposed for a little more than a month.

Wet density, dry density, and moisture content of soils were determined *in situ* using a Campbell Pacific Nuclear 501DR portable probe. The probe contains a gamma source and a gamma-measuring detector for density measurements, and a

fast neutron source and thermal neutron detector for moisture measurements.

Soil texture was estimated for sites where soil-gas samples were collected. Where possible, estimates were based on soil from the depth of gas-sample collection. The soil texture was classified into one of twelve categories used by the U.S. Soil Conservation Service (1975). Classification is based on the less than 2-millimeter (0.08-in) fraction, and is modified by estimates of the volume percent of gravel.

Indoor-radon levels for both the statewide and targeted surveys were measured with ATDs placed in the lowest occupied living space of single-family, owner-occupied homes, as well as in basement rooms of selected schools, or ground-floor rooms of schools without basements. Nineteen detectors were allotted for each school, however some detectors were lost or damaged during the monitoring period. School testing was conducted during the 1990/91 school year in accordance with EPA guidance, which suggests normal school-room occupancy and normal operating procedures for central heating, ventilation, and air conditioning systems during the measurement period (U.S. Environmental Protection Agency, 1989). Duplicate detectors were used to analyze the precision of school measurements, and field blanks (control detectors) were used to determine the extent of exposure to extraneous radiation sources.

Data and Discussion

Uranium levels from the ground-spectrometer survey are significantly higher in the east Sandy area (5.6 ppm) (table 1) than in the east Provo area (2.6 ppm) (table 2). The distribution of uranium in the two areas, however, is not uniform. In east Sandy, the highest average uranium levels are in upper Pleistocene deltaic deposits of the Provo (regressive) shoreline of the Bonneville lake cycle (7.1 ppm). Uranium levels in upper Pleistocene gravelly alluvium of terraces graded to the Provo shoreline are bimodally distributed; lower levels (4.1 ppm) occur west of the mouth of Big Cottonwood Canyon, whereas higher levels (6.9 ppm) are present elsewhere. In east Provo, the highest average uranium levels are in upper Pleistocene lacustrine gravel of the Bonneville (transgressive) shoreline (3.1 ppm). The distribution of total gamma, eTh, and K parallels that of eU in east Sandy and is consistent with a siliceous igneous rock source (Nielson and others, 1991) (tables 3 and A-3). In east Provo, eU is more concentrated relative to both eTh and K in areas of high eU anomalies, indicating a significant contribution from non-igneous sources (tables 4 and A-4).

Average levels of radon in soil gas from the scintillometer survey are also higher in east Sandy (528 pCi/L [1.95 x 10^4 Bq/m^3]) (table 1) than in east Provo (449 pCi/L [1.66 x 10^4 Bq/m^3]) (table 2). In east Sandy, the highest average levels of radon in soil gas are in the upper Pleistocene terrace deposits noted above (641 pCi/L [2.37 x 10^4 Bq/m^3]). Average levels are lower in the Bonneville shoreline lacustrine gravel (565 pCi/L [2.09 x 10^4 Bq/m^3]), but levels are lowest where the gravel occurs west of the mouth of Big Cottonwood Canyon (296 pCi/L [1.10 x 10^4 Bq/m^3]) compared to similar deposits elsewhere in east Sandy (654 pCi/L [2.42 x 10^4 Bq/m^3]). In east Provo, the highest levels of radon in soil gas are in middle Holocene to upper Pleistocene alluvial fans (679 pCi/L [2.51 x 10^4 Bq/m^3]).

Soil-gas radon measurements from both the east Sandy and east Provo areas are lognormally distributed with many samples of a relatively low concentration, but a few samples with high concentrations (figure 11). This is expected when trace elements, such as radon, are randomly distributed in a homogenous material (Rogers, 1964). Therefore, unconsolidated material in the study areas can be considered homogenous, although inhomogeneities are evident when the material is subdivided into geologic units. However, the correlation between soil-gas radon and surface-uranium concentrations measured at the same sites, although statistically significant, shows considerable scatter (figure 12). The regression line shown in figure 12 was forced to zero and was determined for a sample size of 113. At the 99 percent confidence level, the correlation coefficient of 0.574 exceeds the threshold value of 0.241. The correlation is improved by not forcing the regression to zero, but this is not realistic because there should be essentially no decay product (Rn) if uranium is absent. Additional soil-gas radon concentrations were measured with ATDs to validate the scintillometer readings. The area selected for validation included both the highest soil-gas (figure 13) and indoor-radon concentrations

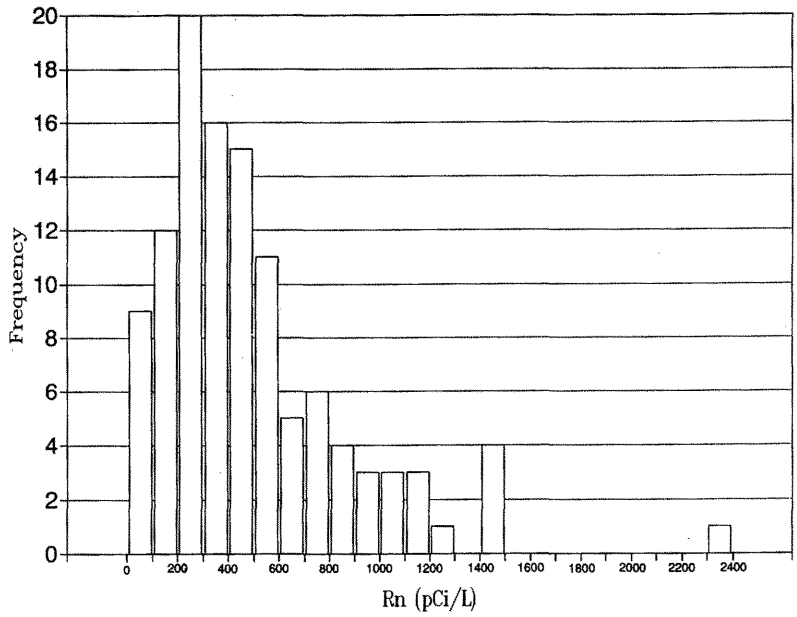

Figure 11. Histogram of soil-gas radon concentrations from the ground-scintillometer surveys in both the east Sandy and east Provo areas. The distribution of concentrations is log-normal, as expected.

Table 3.

Statistical summary of additional ground-radiometric data in the east Sandy area. Geologic units were mapped by Personius and Scott (1990, 1992) (figure 2), but units ca, alp, and lbg have been subdivided where they occur on the Big Cottonwood and Little Cottonwood deltas. N is the number of sample sites.

Geologic Unit	N	Total Counts		K		eTh		eU/eTh	
		Avg. ppm	Max. ppm	Avg. %	Max. %	Avg. ppm	Max. ppm	Avg.	Max.
Lacustrine Deposits									
Deposits postdating the Bonneville lake cycle									
Lacustrine, marsh, and alluvial deposits (laly)	2	12.6	13.3	1.6	1.8	9.9	10.5	0.32	0.36
Regressive-phase deposits of Bonneville lake cycle									
Deltaic deposits (lpd)	7	22.9	28.3	2.4	3.2	12.5	15.0	0.57	0.76
Lacustrine gravel (lpg)	33	19.5	27.4	2.4	3.8	12.2	17.5	0.40	0.79
Transgressive-phase deposits of Bonneville lake cycle									
Lacustrine gravel (lbg)	17	18.8	24.2	2.3	2.9	12.9	16.9	0.39	0.73
Big Cottonwood	2	20.9	24.2	2.1	2.5	11.4	12.0	0.62	0.72
Little Cottonwood	15	18.5	23.4	2.3	2.9	13.1	16.9	0.36	0.73
Undivided deposits of Bonneville lake cycle									
Lacustrine clay and silt (lbpm)	2	17.2	19.3	2.1	2.1	12.6	14.0	0.31	0.46
Alluvial Deposits									
Stream alluvium									
Unit 1 (al1)	6	23.1	25.5	2.6	3.1	15.0	19.0	0.49	0.75
Unit 2 (al2)	1	15.4	15.4	1.7	1.7	11.6	11.6	0.32	0.32
Regressive-phase alluvium (alp)	34	22.6	28.0	2.5	3.2	13.9	18.8	0.49	0.90
Big Cottonwood	2	14.5	16.7	1.6	1.6	10.6	11.2	0.38	0.49
Little Cottonwood	32	23.1	28.0	2.6	3.2	14.1	18.8	0.50	0.90
Fan alluvium									
Unit 1 (af1)	1	19.0	19.0	2.6	2.6	14.3	14.3	0.29	0.29
Unit 2 (af2)	6	18.9	27.3	2.4	3.4	15.6	20.6	0.27	0.42
Glacial Deposits									
Outwash of Bells Canyon age (gbco)	2	24.9	25.6	2.7	2.9	15.3	16.8	0.47	0.54
Till of Bells Canyon age (gbct)	2	23.1	25.5	2.9	3.3	15.9	17.0	0.36	0.37
Eolian Deposits									
Sand (es)	8	20.5	26.2	2.5	2.9	12.2	16.2	0.43	0.64
Colluvial Deposits									
Debris-flow deposits 1 (cd1)	0	–	–	–	–	–	–	–	–
Hillslope colluvium (chs)	2	21.5	23.7	2.9	3.4	14.9	17.5	0.39	0.46
Colluvium and alluvium (ca)	8	19.6	26.1	2.2	2.6	13.5	17.2	0.43	0.53
Big Cottonwood	4	18.3	26.1	2.0	2.6	13.4	17.2	0.40	0.49
Little Cottonwood	4	20.9	24.3	2.4	2.5	13.6	14.8	0.46	0.53
Fill Deposits									
Man-made fill (f)	0	–	–	–	–	–	–	–	–
EAST SANDY TOTAL	131	20.6	28.3	2.4	3.8	13.2	20.6	0.43	0.90

Table 4.

Statistical summary of additional ground-radiometric data in the east Provo area. Geologic units were mapped by Machette (1989) (figure 3). N is the number of sample sites.

Geologic Unit	N	Total Counts		K		eTh		eU/eTh	
		Avg. ppm	Max. ppm	Avg. %	Max. %	Avg. ppm	Max. ppm	Avg.	Max.
Lacustrine Deposits									
Regressive-phase deposits of Bonneville lake cycle									
Deltaic deposits (lpd)	2	8.3	9.1	1.1	1.2	6.5	6.6	0.32	0.33
Lacustrine gravel (lpg)	3	7.7	8.4	1.1	1.1	5.6	6.3	0.33	0.38
Lacustrine sand (lps)	4	9.2	10.3	1.1	1.2	6.5	7.0	0.36	0.42
Lacustrine silt and clay (lpm)	0	–	–	–	–	–	–	–	–
Transgressive-phase deposits of Bonneville lake cycle									
Lacustrine gravel (lbg)	2	10.4	11.0	1.3	1.3	8.1	8.4	0.39	0.49
Lacustrine sand (lbs)	9	10.5	13.9	1.3	1.6	8.6	12.2	0.33	0.52
Lacustrine silt and clay (lbm)	10	9.5	12.4	1.1	1.7	7.2	10.2	0.41	0.52
Alluvial Deposits									
Stream alluvium									
Unit 1 (al1)	2	9.7	12.7	1.1	1.4	6.7	8.1	0.43	0.49
Unit 2 (al2)	8	8.5	11.0	1.1	1.3	6.3	8.9	0.40	0.55
Regressive-phase alluvium (alp)	24	8.9	11.2	1.2	1.7	6.8	9.2	0.37	0.90
Fan alluvium									
Unit 2 (af2)	8	9.2	11.8	1.2	1.3	6.7	9.7	0.40	0.64
Younger fan alluvium (afy)	19	9.3	14.1	1.1	1.8	6.4	9.4	0.46	0.68
Regressive-phase fan alluvium (afp)	6	9.6	10.5	1.2	1.3	6.3	7.5	0.44	0.55
Transgressive-phase fan alluvium (afb)	0	–	–	–	–	–	–	–	–
Unit 4 (af4)	0	–	–	–	–	–	–	–	–
Eolian Deposits									
Sand and silt (es)	2	8.4	9.4	1.2	1.4	6.2	6.4	0.28	0.29
Colluvial Deposits									
Older landslide deposits (clso)	0	–	–	–	–	–	–	–	–
EAST PROVO TOTAL	99	9.2	14.1	1.2	1.8	6.8	12.2	0.39	0.90

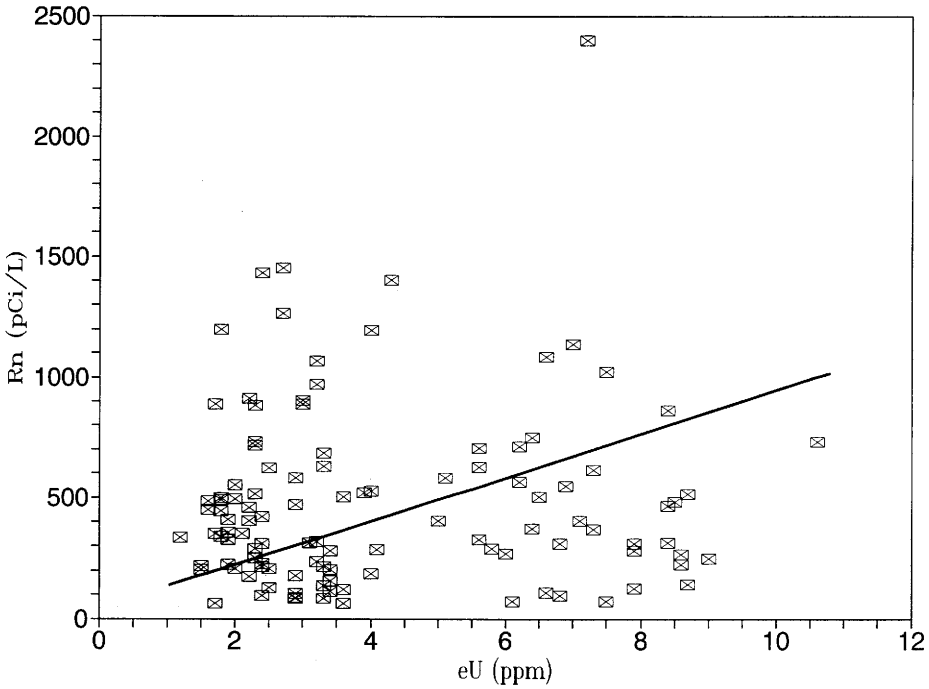

Figure 12. *Scatter plot and linear regression, with regression line forced to zero, of uranium from the ground-spectrometer survey and soil-gas radon from the ground-scintillometer survey. The regression line was determined for a sample size of 113. At the 99 percent confidence level, the correlation coefficient of 0.574 exceeds the threshold value of 0.241.*

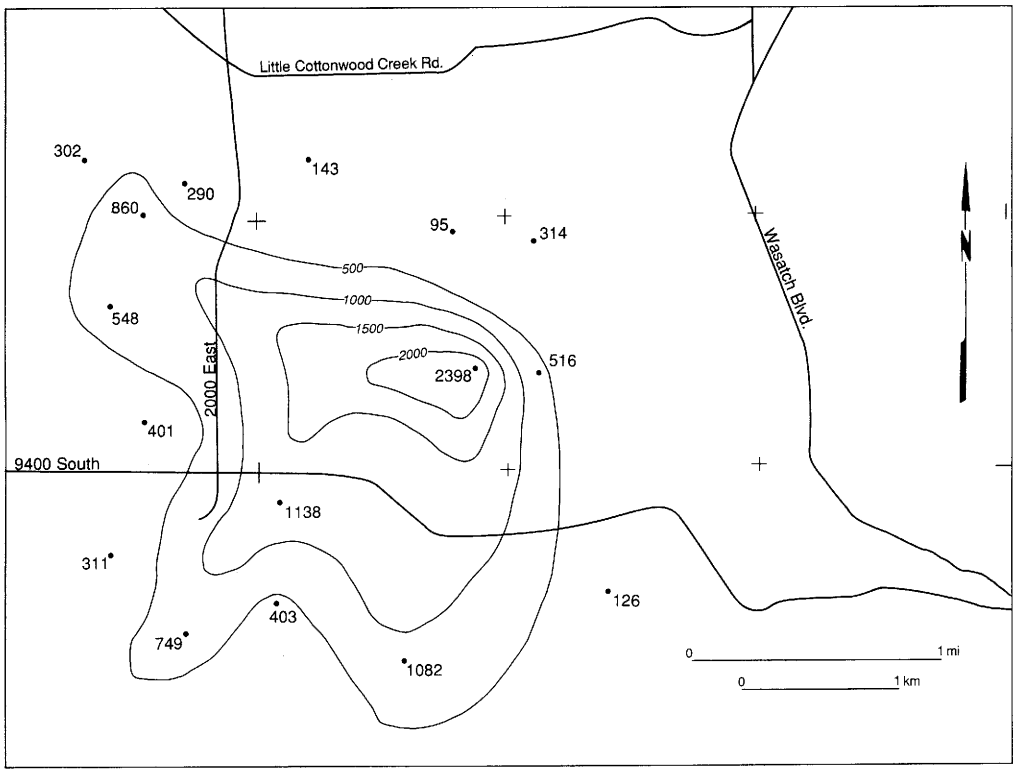

Figure 13. *Contour map of anomalous concentrations of radon in soil gas, east Sandy "hot spot," from the ground-scintillometer survey. Contour interval 500 pCi/L (1.85 x 10^4 Bq/m^3).*

(figure 14) in the east Sandy area. This east Sandy "hot spot," an area of over 4 square miles (10 km^2), has an average indoor-radon level of 9.1 pCi/l (337 Bq/m^3). Of 28 indoor measurements in the "hot spot," all were greater than 4 pCi/L (148 Bq/m^3), with a maximum measurement of 26.2 pCi/L (969 Bq/m^3).

ATD field measurements (table 5) were made at three different times in the Sandy area: December, 1990; late March and early April, 1991; and May, 1991. The December and March-April measurements sampled gas concentrations at the same general sites, although different holes and depths were used, to evaluate the reproducibility of results and to standardize for variations in atmospheric conditions. Atmospheric conditions, particularly precipitation and temperature, profoundly affect soil-gas radon levels. Much radon variability occurs in annual cycles because soil-moisture content, and radon partitioning between gas and water, are temperature sensitive. In central Pennsylvania, soil-gas radon concentrations to a depth of 2 meters (7 ft) varied in an annual cycle by a magnitude of ten (Washington and Rose, 1992). The results of the December and March-April surveys, depth corrected, are evaluated graphically on figure 15 using least-squares regression. The calculated correlation coefficient indicates a good linear relationship between the two data sets, although soil-gas radon concentrations are almost uniformly higher in late fall measurements than in those made in the early spring. The sample size is 9. At the 99 percent confidence level, the correlation coefficient of 0.849 exceeds the threshold value of 0.798.

Field and laboratory ATD measurements are directly related (figure 16), showing that field ATDs measure locally derived radon rather than gas that has migrated some distance from another source. The relationship is non-linear because of insufficient laboratory measurement time for the samples to reach equilibrium. However, field measurements can be used to characterize the radon-hazard potential of Quaternary geologic units.

Anomalously high values of soil-gas radon were measured in the same area during both the scintillometer (figure 13) and ATD surveys (figures 17 through 20). The details of the distribution and magnitude are different due to variations in sampling locations and atmospheric conditions during the sampling intervals. A high value of 2,398 pCi/L (8.87×10^4 Bq/m^3) detected by the scintillometer survey was not confirmed by the ATD surveys, although the scintillometer sample site was not reoccupied for ATD testing because of difficulty in excavating a suitable hole in gravel for proper ATD placement. A localized concentration of radon-generating material cannot be ruled out. However, elevated soil-gas radon levels at the scintillometer site are apparently real because this sample was collected on the grounds of Quail Hollow Elementary School which, with adjacent Albion Middle School, have elevated levels of indoor radon as well (table 6 and figure 14). The anomaly is restricted to upper Pleistocene gravelly alluvium in terraces graded to the Provo (regressive) shoreline, and gravel of the Bonneville (transgressive) shoreline. The radon anomaly corresponds to material near the mouth of Little Cottonwood Canyon derived from uranium-enriched granitic rocks. Radon levels are lower in material near the mouth of Big Cottonwood Canyon derived from uranium-deficient metasedimentary rocks.

Soil permeability affects the rate of soil-gas migration and can be estimated from measurements of moisture, porosity, and particle diameter (Rogers and Nielson, 1990). An attempt was made to measure moisture and density, from which porosity may be calculated, with a moisture-density gauge. However, gravelly soil commonly prevented the necessary access holes from being augered. The few moisture and density measurements made are biased toward sample sites with finer-grained soils. Soil permeability may also be estimated from the textural classification of the soil. Because soil texture did not significantly change between geologic units, permeability estimates of the various units within each area were not attempted. However, soils from east Sandy are generally gravelly sands and are more permeable than the abundant gravelly muddy sands of the east Provo area.

Pore water traps radon and inhibits its migration in soil gas. Conversely, unsaturated porosity facilitates diffusion of radon to the atmosphere. This phenomenon is evident in east Sandy. Most Quaternary units near Big Cottonwood Canyon have lower uranium concentrations than similar units near Little Cottonwood Canyon. However, a few poorly drained (wet) Quaternary units near Big Cottonwood Canyon have high uranium concentrations but low levels of radon in soil gas (see units lpd, al1, and ca on figure 21). Well-drained (dry), transgressive-phase lacustrine gravel deposits (unit lbg, figure 21) near Little Cottonwood Canyon have lower uranium concentrations than their poorly drained counterparts near Big Cottonwood Canyon, but have higher soil-gas radon levels. The relationship between ground water and radon is not as clear in east Provo, possibly because uranium levels are lower and there is a smaller contrast between uranium levels of different geologic units (figure 22). The degree of pore saturation in the survey areas is estimated by tabulating the number of sample sites in each geologic unit with ground-water depths greater than 50 feet (15 m) (tables 1 and 2) (Anderson and others, 1986a, 1986b). Poorly drained geologic units have fewer sample sites with deep ground water than do well-drained units. The 50-foot (15-m) depth does not necessarily indicate a threshold that affects radon migration or diffusion.

Levels of indoor radon are affected by the geologic factors, and reflect differences in these factors between the various geologic units in the two study areas (tables 1, 2, and 6). The highest average indoor-radon levels in both areas occur in houses and schools on upper Pleistocene deposits of the Bonneville (transgressive) shoreline, and in overlying units. In east Sandy these deposits are predominantly gravel and have an average indoor-radon level of 3.5 pCi/L (130 Bq/m^3); homes and schools west of the mouth of Big Cottonwood Canyon have lower indoor-radon levels than homes and schools near Little Cottonwood Canyon. Deposits with the highest average indoor-radon levels in east Provo are predominantly silt and clay and average 3.7 pCi/L (137 Bq/m^3). In both areas, geologic units with high average indoor-radon levels are commonly characterized by relatively high levels of uranium and soil-gas radon, as well as deeper ground-water levels (tables 1 and 2). Geologic units with low average indoor-radon levels are commonly characterized by relatively low levels of uranium and soil-gas radon; however, poorly drained uraniferous units also commonly have low levels of soil-gas and indoor radon.

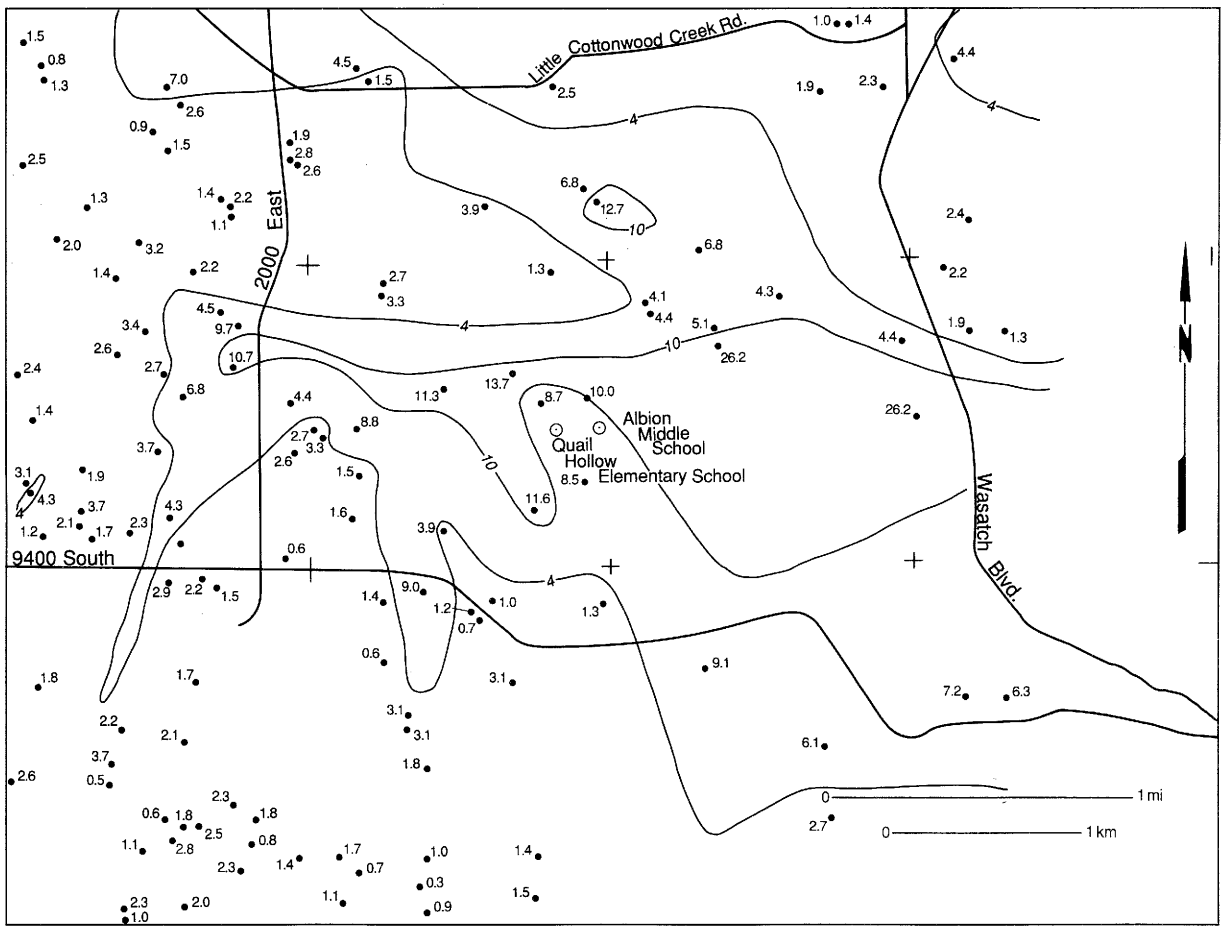

Figure 14. *Contour map of indoor-radon concentrations, east Sandy "hot spot." Contours at 4 and 10 pCi/L (148 and 370 Bq/m^3).*

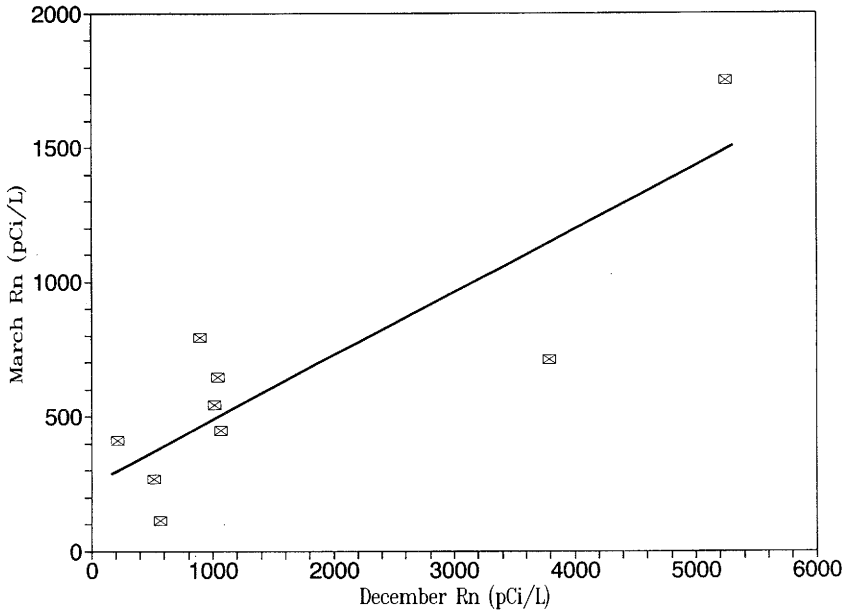

Figure 15. *Linear regression of radon in soil gas, depth-corrected, measured in field with alpha-track detectors. Samples were collected at the same sites during two time intervals, and late fall values are uniformly higher than those measured in early spring. The regression line was determined for a sample size of 9. At the 99 percent confidence level, the correlation coefficient of 0.849 exceeds the threshold value of 0.798.*

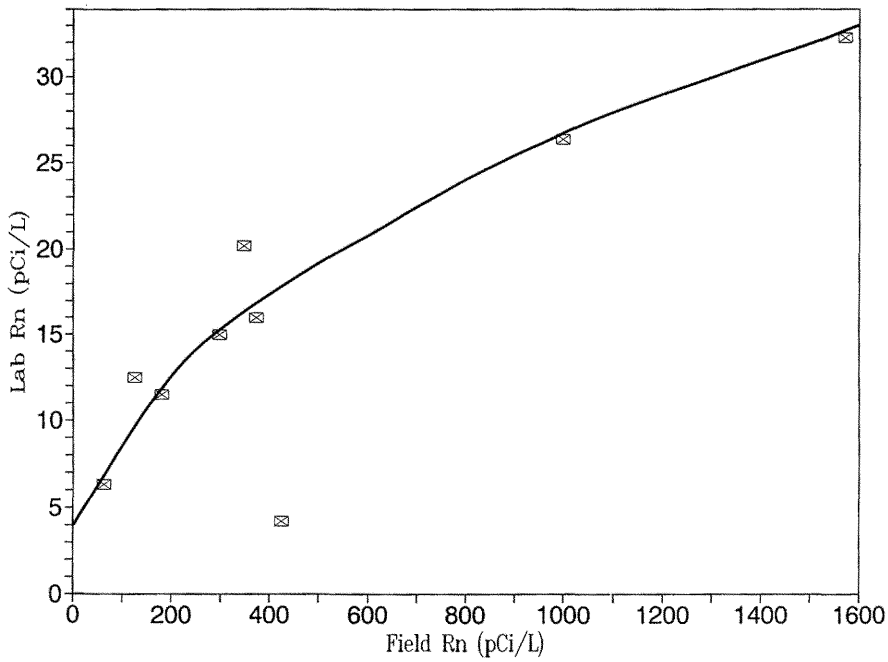

Figure 16. *The relationship between field and laboratory measurements of radon in soil gas. The smooth curve suggests that field measurements of soil-gas radon represent radon that is locally derived, rather than gas that has migrated some distance from other source materials. The non-linearity results from insufficient measurement time for the laboratory samples to reach equilibrium.*

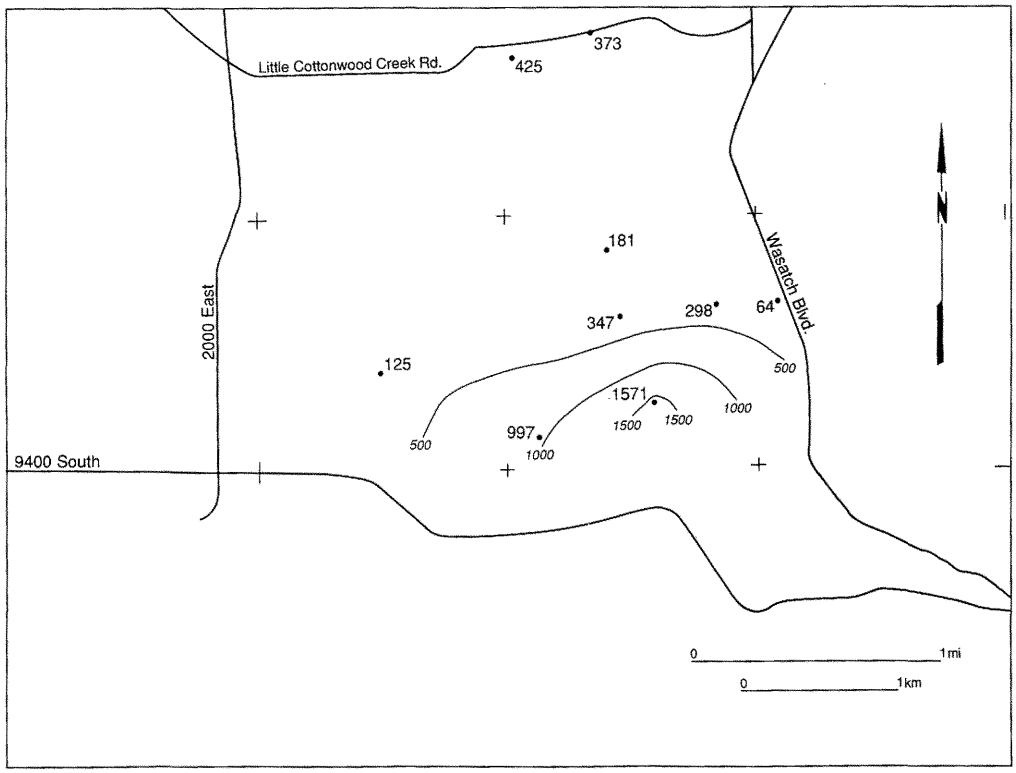

Figure 17. *Contour map of soil-gas radon measured in the field with alpha-track detectors during December, 1990. Contour interval 500 pCi/L (1.85 x 10^4 Bq/m^3).*

Table 5.

Soil-gas radon measurements from ATDs, collected in situ (Field Rn) and from laboratory analysis (Lab Rn). Depth-corrected in situ measurements are also listed. In situ measurements, both depth-corrected and uncorrected, are plotted in figures 17 through 20.

Station	Date	Field Rn pCi/L	Lab Rn pCi/L	Depth cm	Depth-corrected concentration pCi/L	Moisture %
DLN-1	12/11-13/90	64.2	6.3	35.6	214.3	1
	03/18-21/91	144.3	--	43.2	411.4	--
DLN-2	12/11-13/90	298.6	15.0	40.6	894.8	9
	03/18-21/91	315.8	--	50.8	792.9	--
DLN-3	12/11-13/90	372.8	16.0	45.7	1,016.3	8
	03/18-21/91	207.8	--	48.3	542.5	--
DLN-4	03/18-21/91	235.7	--	43.2	671.9	--
DLN-5	12/11-13/90	424.6	4.2	50.8	1,066.0	19
	03/18-21/91	157.0	--	43.2	447.6	--
DLN-6	12/11-13/90	347.4	20.2	40.6	1,041.1	8
	03/18-21/91	236.2	--	45.7	643.9	--
DLN-7	12/11-13/90	180.9	11.5	38.1	571.0	3
	03/18-21/91	36.0	--	38.1	113.6	--
DLN-8	12/11-13/90	996.8	26.4	30.5	3,791.9	3
	03/19-21/91	249.5	--	43.2	711.3	--
DLN-9	12/11-13/90	1,571.3	32.3	35.6	5,245.9	4
	03/19-21/91	613.9	--	43.2	1,750.0	--
	05/05-08/91	135.7	--	35.6	453.0	--
DLN-10	12/11-13/90	125.3	12.5	27.9	514.7	1
	03/19-21/91	93.2	--	43.2	265.7	--
DLN-11	05/05-08/91	154.3	--	27.9	633.8	--
DLN-12	05/05-08/91	123.0	--	27.9	505.2	--
DLN-13	05/05-08/91	321.4	--	27.9	1,320.1	--
DLN-14	05/05-08/91	104.2	--	27.9	428.0	--
DLN-15	05/05-08/91	103.5	--	30.5	393.7	--
DLN-16	05/05-08/91	107.9	--	38.1	340.6	--
SJL-1	03/19-21/91	203.1	--	43.2	579.0	--
	03/29-04/01/91	272.5	--	40.6	816.6	--
SJL-2	03/19-21/91	315.8	--	38.1	996.8	--
SJL-3	03/19-21/91	912.9	--	43.2	2,602.4	--
SJL-4	03/29-04/01/91	540.6	--	40.6	1,620.1	--
SJL-5	03/29-04/01/91	402.4	--	45.7	1,097.0	--
SJL-6	03/29-04/01/91	432.1	--	45.7	1,178.0	--
SJL-7	03/29-04/01/91	734.2	--	45.7	2,001.5	--
SJL-8	03/29-04/01/91	426.7	--	45.7	1,163.2	--
SJL-9	03/29-04/01/91	418.2	--	43.2	1,192.2	--
SJL-10	03/29-04/01/91	703.6	--	43.2	2,005.8	--
SJL-11	03/29-04/01/91	331.4	--	45.7	903.4	--
SJL-12	03/29-04/01/91	690.4	--	45.7	1,882.1	--
SJL-13	03/29-04/01/91	251.1	--	38.1	792.6	--
SJL-14	03/29-04/01/91	244.3	--	43.2	696.4	--
SJL-15	03/29-04/01/91	452.1	--	38.1	1,427.0	--

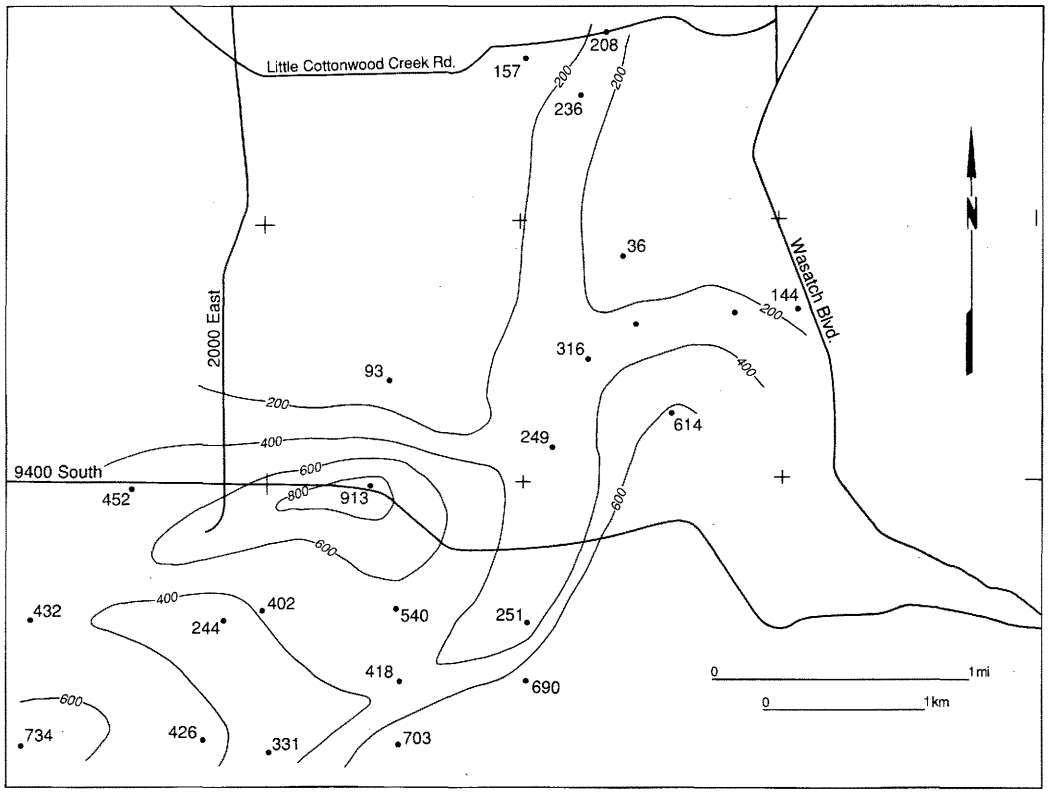

Figure 18. *Contour map of soil-gas radon measured in the field with alpha-track detectors during March and April, 1991. Contour interval 200 pCi/L (7.4 x 10^3 Bq/m^3). Radon levels are generally lower than in December, 1990 (figure 17).*

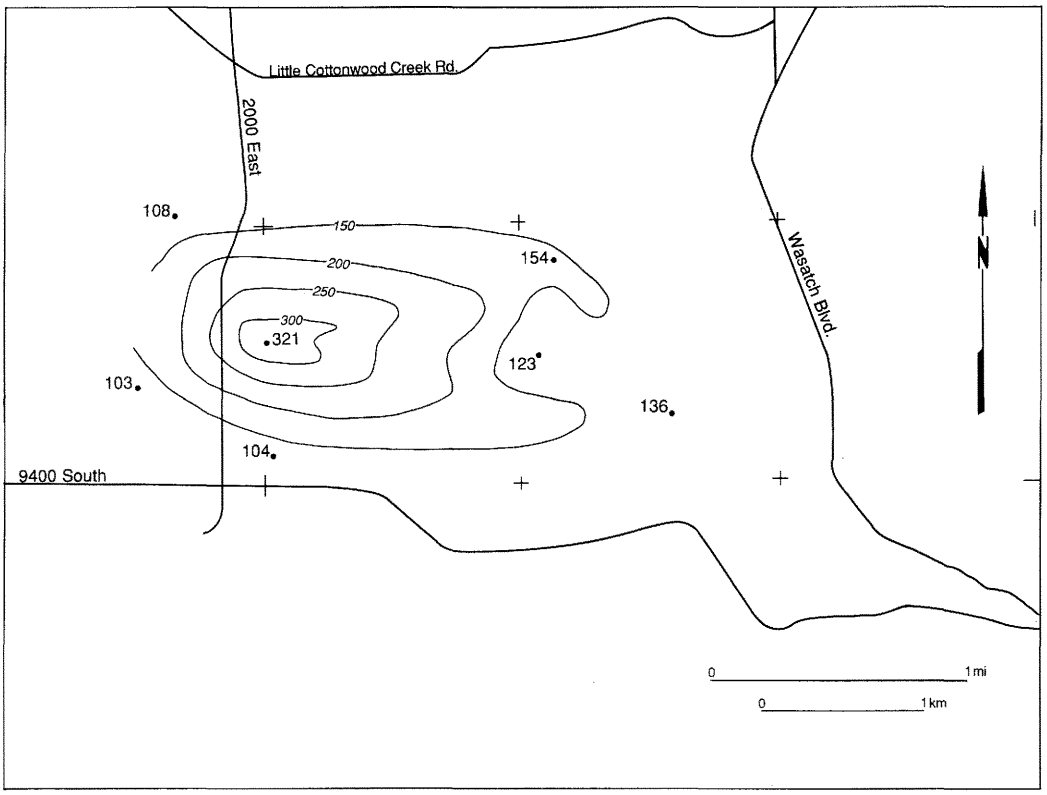

Figure 19. *Contour map of soil-gas radon measured in the field with alpha-track detectors during May, 1991. Contour interval 50 pCi/L (1.85 x 10^3 Bq/m^3). Radon levels have continued their decline beyond March and April measurements (figure 18).*

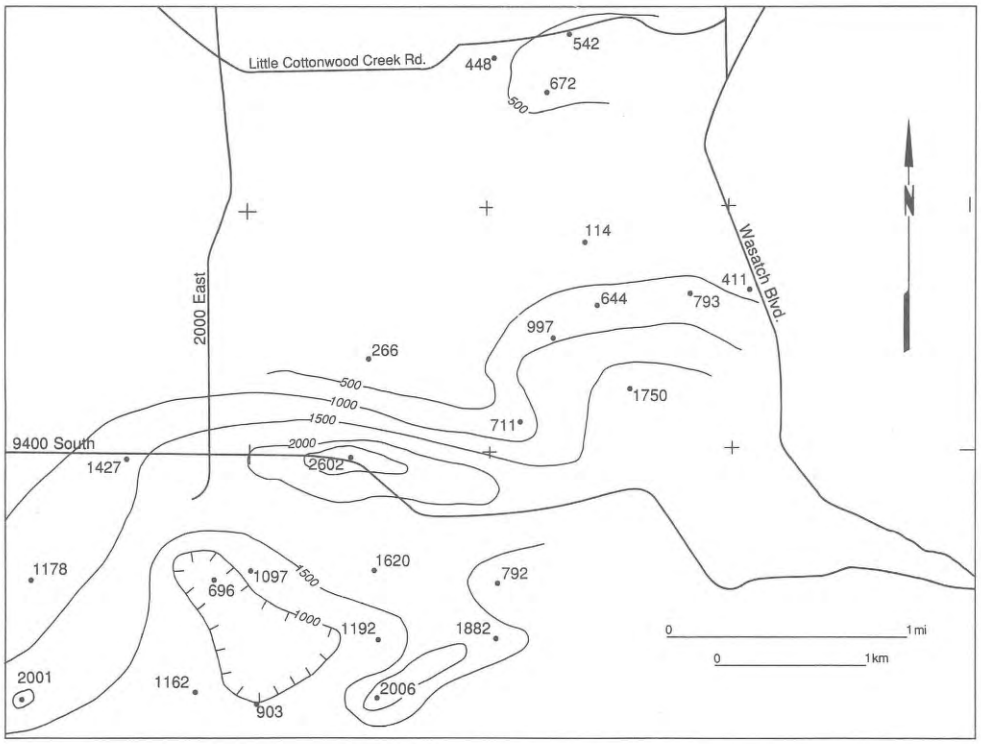

Figure 20. *Contour map of depth-corrected soil-gas radon measured in the field with alpha-track detectors during March and April, 1991. Contour interval 500 pCi/L (1.85 x 10^4 Bq/m^3).*

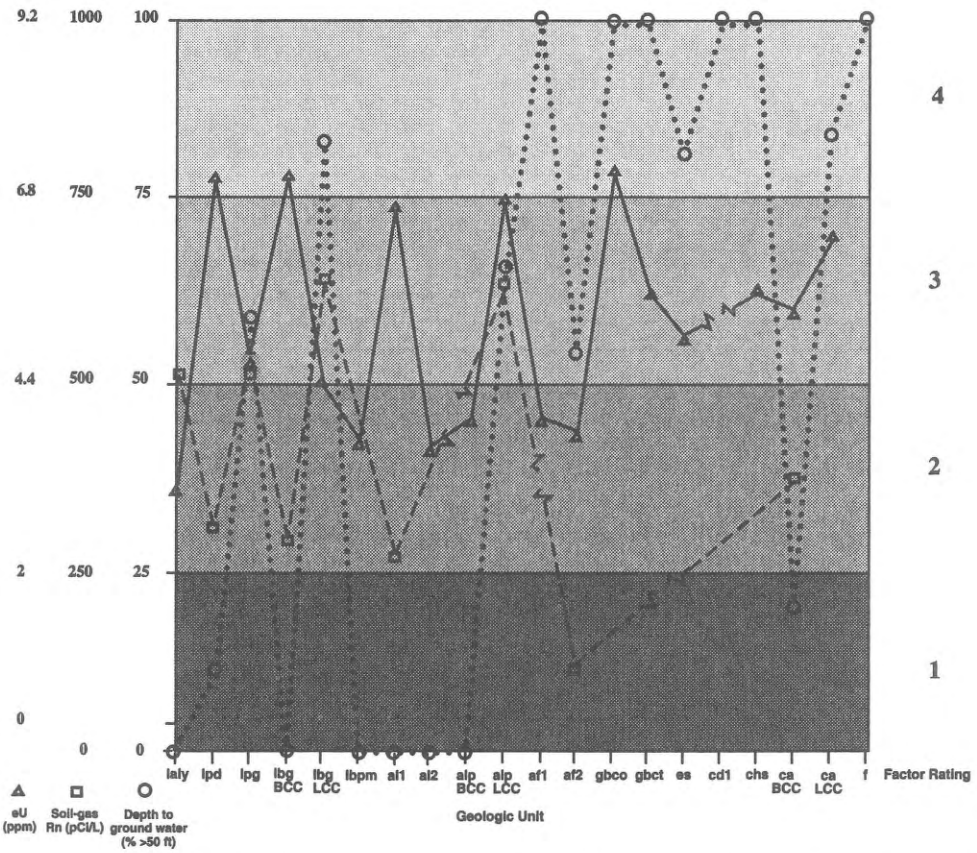

Figure 21. *Average levels of hazard-rating factors in Quaternary geologic units of the east Sandy area. These are the factors used to compile the potential-radon-hazard ratings in table 1; factor ratings are shown at right. The lines which connect the symbols are for clarity and do not imply a spatial relationship between the units. See table 1 for explanation of geologic units.*

Table 6.

Summary of indoor-radon measurements in selected schools, Jordan School District (east Sandy study area) and Provo School District (east Provo study area). Quail Hollow and Albion Schools have rooms with elevated indoor-radon levels, and are located in the east Sandy "hot spot" (figure 14), a high-hazard area (figure 25). Canyon Crest Elementary School also has rooms with elevated indoor-radon levels, and is in a moderate-hazard area of east Provo (figure 26). N is the number of measurements that fall within specified ranges, and does not include the results of duplicate or control detectors.

Location	<4 pCi/L		4-10 pCi/L		>10 pCi/L	
	N	%	N	%	N	%
Albion Middle School	5	29.4	10	58.8	2	11.8
Brighton High School	18	100.0	0	0.0	0	0.0
Butler Elementary	17	100.0	0	0.0	0	0.0
Canyon View Elementary	16	100.0	0	0.0	0	0.0
Cottonwood Heights Elementary	17	100.0	0	0.0	0	0.0
Eastmont Middle School	17	100.0	0	0.0	0	0.0
Granite Elementary	16	100.0	0	0.0	0	0.0
Lone Peak Elementary	17	100.0	0	0.0	0	0.0
Mountainview Elementary	17	100.0	0	0.0	0	0.0
Quail Hollow Elementary	11	57.9	8	42.1	0	0.0
Sunrise Elementary	17	100.0	0	0.0	0	0.0
Willow Canyon Elementary	16	100.0	0	0.0	0	0.0
Jordan School District Total	184	90.2	18	8.8	2	1.0
Canyon Crest Elementary	1	5.6	16	88.9	1	5.6
Farrer Middle School	15	100.0	0	0.0	0	0.0
Provo High School	13	100.0	0	0.0	0	0.0
Sunset View Elementary	18	100.0	0	0.0	0	0.0
Provo School District Total	47	73.4	16	25.0	1	1.6

Table 7.

Radon hazard-potential matrix for the Wasatch Front. Each of three factors are given ratings which range from 1 (lowest potential for contributing to high indoor-radon levels) to 4 (highest potential). Ratings for the three factors are then added, and the composite rating is used to define the three relative hazard-potential categories shown in table 8.

Factor Rating	eU ppm	Soil Rn pCi/L	Ground-water Depth % >50 ft
1	<2.0	<250.0	<25
2	2.0-4.4	250.0-500.0	25-50
3	4.4-6.8	500.1-750.0	51-75
4	>6.8	>750.0	>75

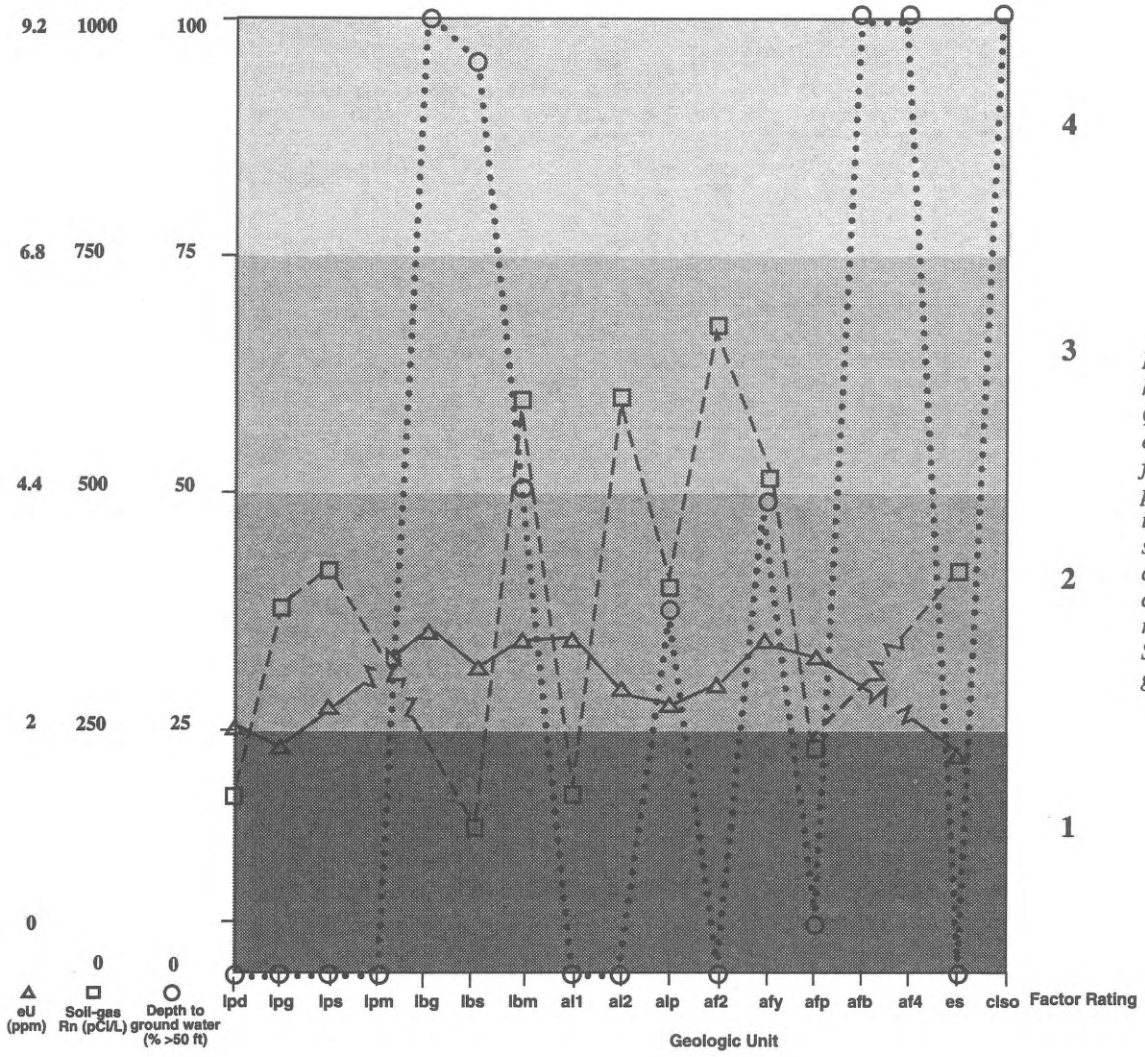

Figure 22. *Average levels of hazard-rating factors in major Quaternary geologic units of the east Provo area. These are the factors used to compile the potential-radon-hazard ratings in table 2; factor ratings are shown at right. The lines which connect the symbols are for clarity and do not imply a spatial relationship between the units. See table 2 for explanation of geologic units.*

Potential Radon Hazard of Quaternary Geologic Units

Three factors are used in this study to estimate the relative radon-hazard potential of geologic units: (1) uranium concentration, (2) soil-gas radon concentration, and (3) ground-water level. Numerical ratings from 1 to 4 were assigned to each factor, with higher ratings corresponding to conditions favorable for elevated indoor-radon concentrations (table 7). Ratings were assigned to uranium and soil-gas radon by constructing normal probability plots (figures 23 and 24) to identify individual data populations bounded by inflection points in the slope of the data. These populations correspond to groups of related geologic units derived from similar sediment-source areas (McCammon, 1980). Ratings were assigned to ground-water by calculating the percentage of sample sites with a depth to ground water of greater than 50 feet (15 m) to identify the relative degree of saturation within geologic units. Ratings for the three factors were summed for each geologic unit and each unit was placed within one of three radon-hazard-potential categories based on the cumulative totals of the three factors (table 8; figures 21 and 22). The factors are equally weighted because there is insufficient data to independently weight them.

The radon-hazard potential of the study areas (figures 25 and 26) is revised from a preliminary version (Solomon and others, 1991) to incorporate statistical correlations between the three hazard-potential factors and additional indoor-testing results. Boundaries between areas of equal hazard potential are modified from contacts of Quaternary geologic units mapped by Machette (1989) (figure 3) and Personius and Scott (1990, 1992) (figure 2). Each geologic unit listed in tables 1 and 2 has a rating that applies to the unit wherever it occurs in each study area, except for three units which are subdivided between occurrences near Big Cottonwood Canyon and Little Cottonwood Canyon in east Sandy. Upper Pleistocene gravelly alluvium of terraces graded to the Provo (regressive) shoreline, upper Pleistocene lacustrine gravel of the Bonneville (transgressive) shoreline, and Holocene to middle Pleistocene colluvium and alluvium have a moderate hazard potential near Big Cottonwood Canyon, but a high hazard potential elsewhere in

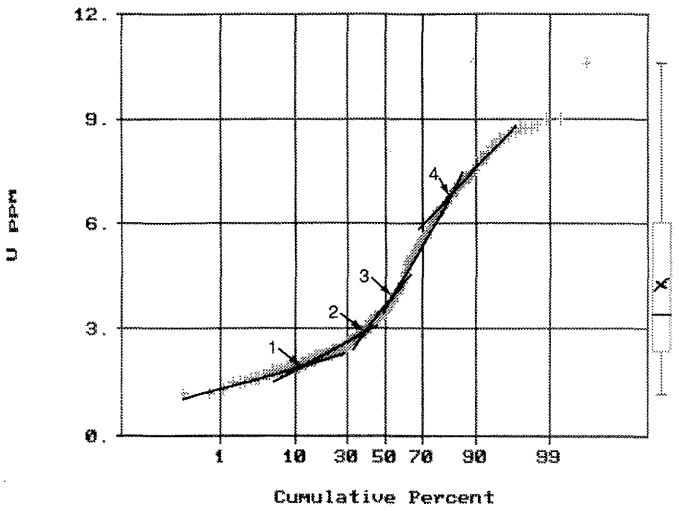

Figure 23. Normal probability diagram of equivalent uranium concentrations. Factor ratings (table 7) are assigned to values bounded by inflection points "1", "3", and "4". Point "3" separates data sets of equal range. There is also an intermediate inflection point "2". The boxplot to the right of the diagram depicts the limits (the ends of the line which extends outward from the rectangle), quartiles (the ends of the rectangle), median (the solid line within the rectangle), and the arithmetic mean (the "X" within the rectangle) of the data set.

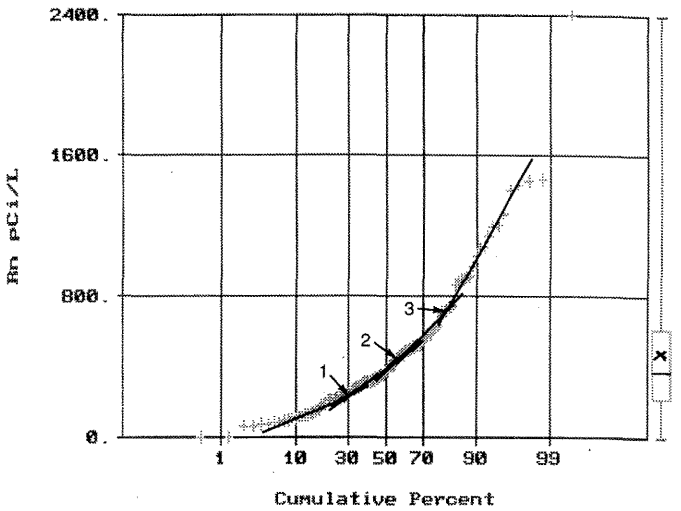

Figure 24. Normal probability diagram of soil-gas radon concentrations measured with the scintillometer. Factor ratings (table 7) are assigned to values bounded by inflection points "1", "2", and "3", which separate data sets of equal range. The boxplot to the right of the diagram depicts statistical values defined for figure 23.

east Sandy. Lower ratings for these units near the mouth of Big Cottonwood Canyon reflect shallower ground water, lower levels of soil-gas radon and, for the terrace deposits and colluvium and alluvium, lower levels of eU at that location. The uranium deficiency is a reflection of source rock within the canyon.

Average values of eU, soil-gas Rn, and ground-water depth in both study areas vary directly with hazard category (low, moderate, and high) (table 9) although average values of these factors for individual geologic units (tables 1 and 2) are more diverse. This is expected because hazard categories reflect the interaction of the three hazard-potential factors, and not the influence of any single factor. Average values of total gamma, K, and eTh also vary directly with hazard category (table 10), but this is coincidental and reflects geochemical variations unrelated to the radon-hazard potential. Variations in hazard potential closely parallel average indoor-radon levels for geologic units with sufficiently large indoor-radon sample sizes (see units lbg and alp near Little Cottonwood Canyon, and lpg, figure 27; and units lbs, lbm, alp, afy, and afp, figure 28), and in several units with small sample sizes. The correlation between hazard potential and indoor-radon levels is imperfect in other units because insufficient data are available. For example, most surveyed indoor-radon levels are high in houses underlain by stream alluvium (unit al2) on the northeastern margin of the east Sandy "hot spot" (figure 14), but the hazard potential of this unit is moderate because only one, relatively low measurement of uranium in soil was collected, and ground water is relatively shallow in the area. Lack of access prevented additional sampling of the unit, but further measurements may indicate either that average uranium values are higher, or that average indoor-radon levels are lower.

Although indoor-radon levels are primarily influenced by the three geologic factors considered in this study, other geologic factors not accounted for may locally influence indoor-radon levels. One such factor is permeability. If geologic materials are sufficiently permeable, soil gas can rapidly diffuse into the atmosphere rather than migrate indoors. This effect may be responsible for the discrepancy between hazard potential and average indoor-radon level for eolian sand (unit es) in east Sandy. The hazard potential of this unit is moderate, and is associated with a high level of uranium and deep ground water. However, the average indoor-radon level in 28 houses overlying this unit is only 1.7 pCi/L (62.9 Bq/m^3). This is the lowest average indoor-radon level of any unit in east Sandy in which more than two indoor levels were measured. Although high levels of soil-gas radon may have been generated by the eolian sand (soil-gas samples could not be collected from this unit because dry sand in access holes collapsed before the probe could be inserted), the soil-gas migrated through the more permeable sand and into the atmosphere, rather than through less permeable foundation material to the house interior.

The interaction of permeability and grain size complicates regional analysis. East Provo has a lower hazard potential than east Sandy, which is confirmed by lower average indoor-radon levels in east Provo. All three geologic factors considered in this study contribute to this difference, but the factor with the largest contrast between the two areas is the uranium content of

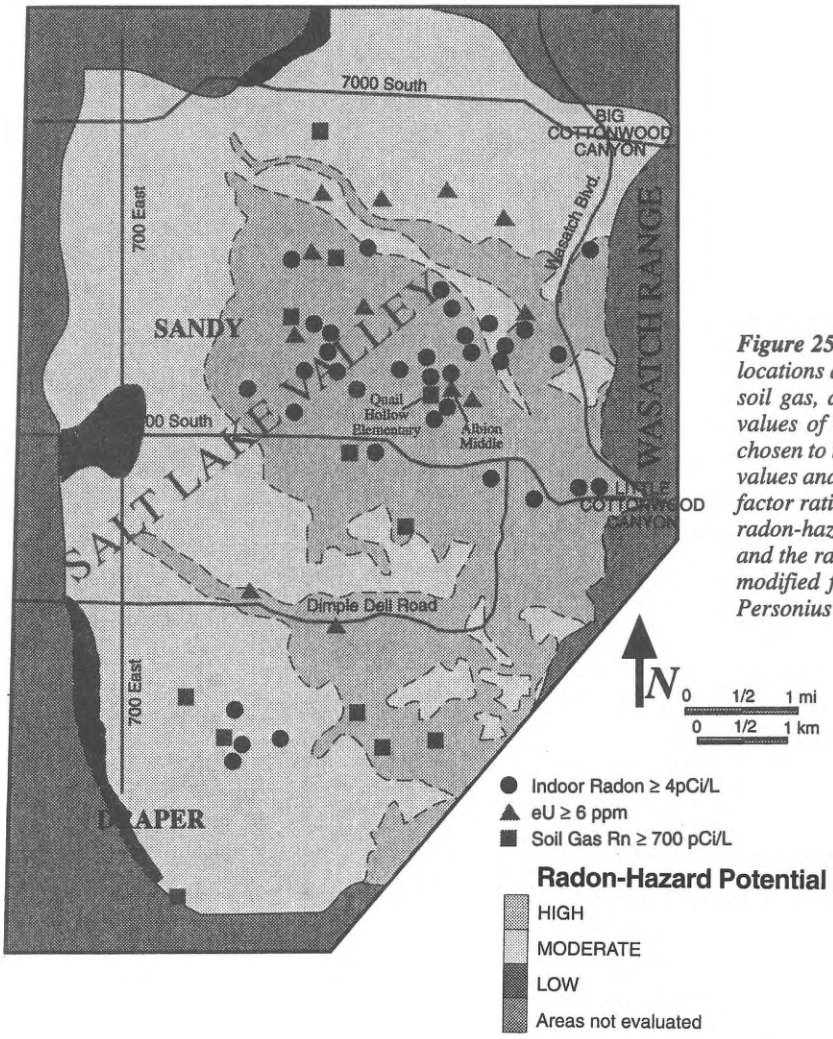

Figure 25. *Map of radon-hazard potential, east Sandy. Approximate locations are shown for measurements of equivalent uranium, radon in soil gas, and indoor radon in excess of threshold values. Threshold values of equivalent uranium and radon in soil gas were arbitrarily chosen to illustrate the geographic relationship between high measured values and hazard ratings, and do not coincide with threshold values of factor ratings in table 7 or with threshold values in figure 21. Areas of radon-hazard potential are based on the data summarized in table 1, and the ratings scheme shown in table 8. Hazard-area boundaries are modified from the contacts of Quaternary geologic units mapped by Personius and Scott (1990, 1992) (figure 2).*

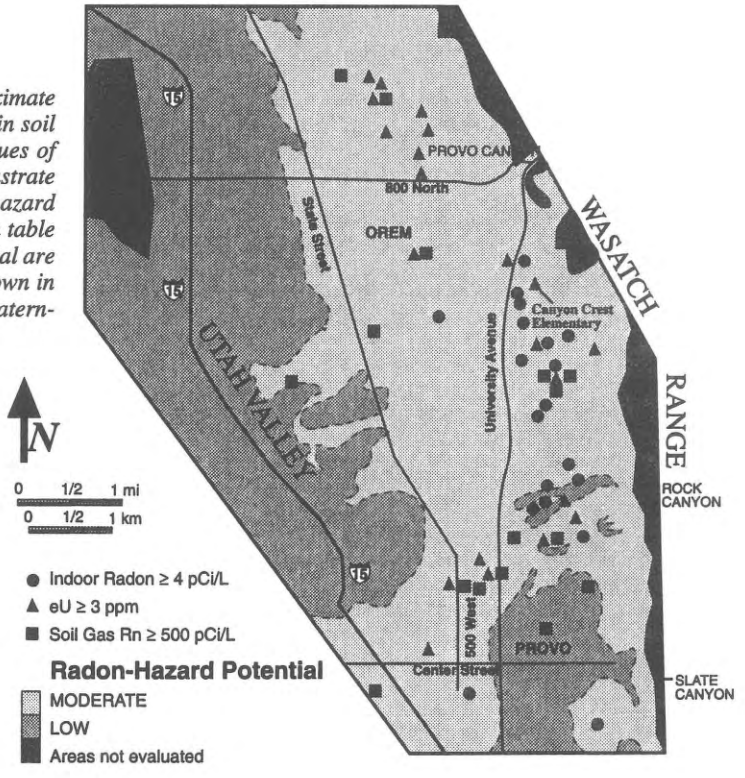

Figure 26. *Map of radon-hazard potential, east Provo. Approximate locations are shown for measurements of equivalent uranium, radon in soil gas, and indoor radon in excess of threshold values. Threshold values of equivalent uranium and radon in soil gas were arbitrarily chosen to illustrate the geographic relationship between high measured values and hazard ratings, and do not coincide with threshold values of factor ratings in table 7 or with threshold values in figure 22. Areas of radon-hazard potential are based on the data summarized in table 2, and the ratings scheme shown in table 8. Hazard-area boundaries are modified from the contacts of Quaternary geologic units mapped by Machette (1989) (figure 3).*

Table 8.
Radon-hazard-potential categories. See table 7 for point value of factors in each category.

Hazard Rating	Hazard Potential
3-5	Low
6-9	Moderate
10-12	High

Table 9.
Statistical summary of field data used as factors to determine radon-hazard-potential categories for Quaternary geologic units. N for eU and soil-gas Rn is the number of sample sites; N for ground-water depth is the number of sites with ground-water depth greater than 50 feet (15 m); N for indoor Rn is the number of sample sites for both this study and the statewide survey (Sprinkel and Solomon, 1990).

Hazard Potential	eU				Rn in soil gas				Depth to ground water		Indoor Rn			
	N	%>3 ppm	Avg. ppm	Max. ppm	N	%>500 pCi/L	Avg. pCi/L	Max. pCi/L	N	%>50 ft	N	%>4 pCi/L	Avg. pCi/L	Max. pCi/L
East Sandy														
Low	2	50	3.8	5.1	2	50	445	580	0	0	1	0	0.8	0.8
Moderate	72	79	5.2	10.6	32	34	453	1,434	85	52	92	8	2.4	26.2
High	57	96	6.2	8.7	22	50	645	2,398	125	74	113	27	3.5	26.2
East Provo														
Low	17	12	2.3	3.6	15	13	323	620	1	2	36	3	1.7	8.1
Moderate	82	29	2.6	4.6	42	38	490	1,463	99	50	116	15	2.8	13.6
High	0	–	–	–	0	–	–	–	0	–	0	–	–	–

Table 10.
Statistical summary of additional ground-radiometric data for radon-hazard-potential categories.

Hazard Potential	N	Total Counts		K		eTh		eU/eTh	
		Avg. ppm	Max. ppm	Avg. %	Max. %	Avg. ppm	Max. ppm	Avg.	Max.
East Sandy									
Low	2	17.2	19.3	2.1	2.1	12.6	14.0	0.31	0.46
Moderate	72	19.8	28.3	2.3	3.8	12.7	20.6	0.42	0.79
High	57	21.7	28.0	2.5	3.4	13.9	18.8	0.45	0.90
East Provo									
Low	17	8.9	10.5	1.1	1.4	6.2	7.5	0.37	0.55
Moderate	82	9.3	14.1	1.2	1.8	6.9	12.2	0.39	0.90
High	0	–	–	–	–	–	–	–	–

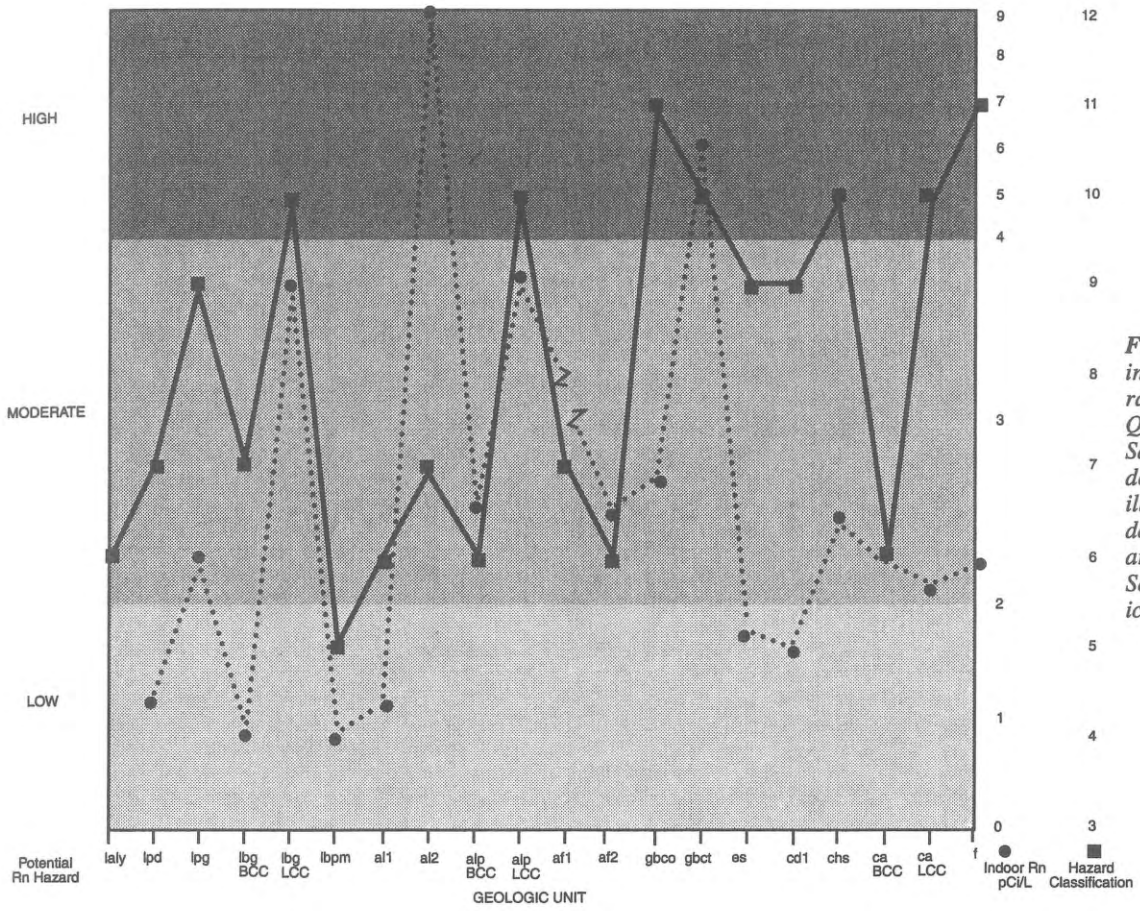

Figure 27. *Comparison of average indoor-radon concentrations and radon-hazard-potential ratings of Quaternary geologic units in the east Sandy area. The vertical scale of indoor radon has been adjusted to illustrate the relationship between indoor-radon concentrations and hazard classification, and is not linear. See table 1 for explanation of geologic units.*

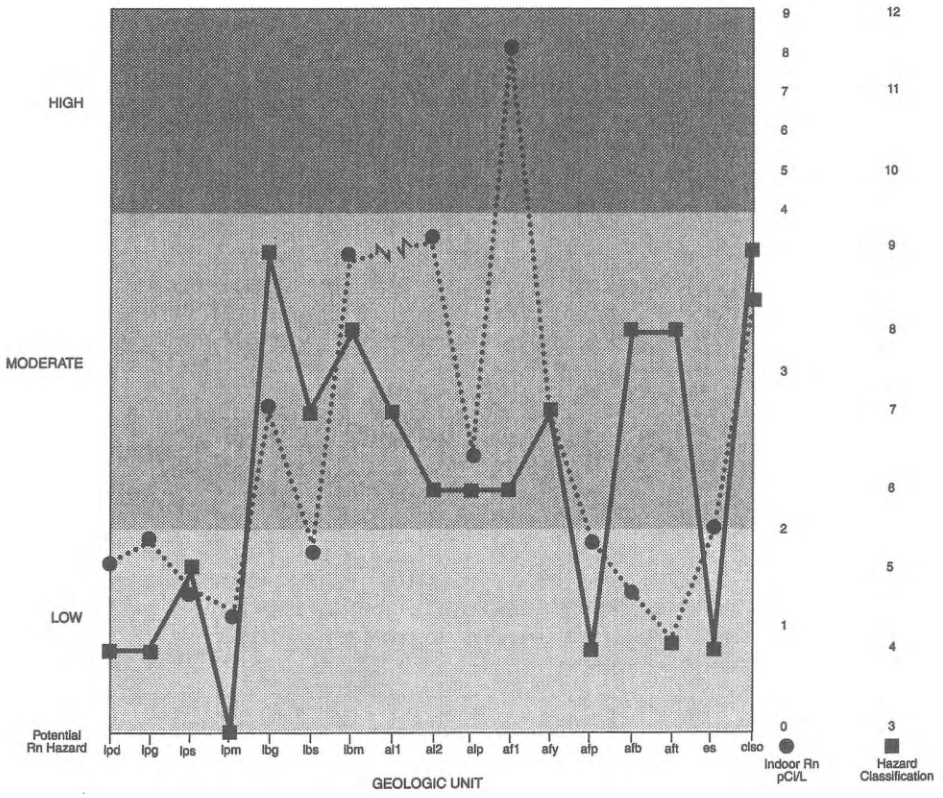

Figure 28. *Comparison of average indoor-radon concentrations and radon-hazard-potential ratings of Quaternary geologic units in the east Provo area. The vertical scale of indoor radon has been adjusted to illustrate the relationship between indoor-radon concentrations and hazard classification, and is not linear. See table 2 for explanation of geologic units.*

soils. However, the difference between the average indoor-radon level of the two areas is less than expected from the difference in uranium content. The average indoor-radon level in east Provo is only 17 percent less than in east Sandy, but the average uranium content in east Provo is 54 percent less. This inconsistency is explained by the process of radon emanation. Radon atoms escape (emanate) more easily from the solid in which they are produced if that solid has a large ratio of surface area to volume (Tanner, 1980). The ratio of surface area to volume increases in finer grained soil. Soils in both east Sandy and east Provo are gravelly, but the soil matrix in east Provo is finer grained than in east Sandy and the emanation process is thus more effective in east Provo. This effect could be taken into account by assigning numerical scores for a "grain size" factor, with the highest score for the finest grain size. Such a factor, though, would contradict the effect of permeability. Greater permeability facilitates radon migration and, hence, the potential for elevated indoor-radon levels. But permeability generally increases with increasing grain size. Thus, if soil texture alone is used as a surrogate for permeability, a high score for permeability in a coarse-grained soil would ignore the effect of surface area and volume. The solution is to use two factors, both grain size and permeability, but direct measurement of permeability is time consuming. Many investigators use permeabilities estimated from percolation tests conducted for U.S. Soil Conservation Service soil surveys (see, for example, Otton and others, 1988). However, soil-survey permeabilities in the east Sandy and east Provo areas (Swenson and others, 1972; Woodward and others, 1974) do not indicate significant permeability contrasts between Quaternary geologic units. The conflicting effects of both permeability and grain size are considered in this study by the inclusion of soil-gas radon as a hazard factor, because levels of soil-gas radon reflect the influence of both permeability and grain size on radon emanation and migration.

Cautions When Using This Report

The hazard ratings presented in this report are not an accurate indicator of actual indoor-radon levels because a quantitative relationship between measured geologic factors and indoor-radon levels does not exist. Important non-geologic factors not considered in this report such as building construction and maintenance techniques, lifestyle, and weather can strongly affect indoor-radon levels within areas of similar radon-hazard potential based on geologic data. The scale of the maps precludes identification of small areas of higher and lower radon-hazard potential contained within the hazard-potential areas depicted on the maps. All map boundaries between hazard-potential areas are approximate due to the gradational nature of geologic contacts. Radon-hazard ratings are relative and are specific only to the east Sandy and east Provo study areas. Indoor-radon statistics in this study are based upon volunteer data, and are not based upon a true random sampling. The use of volunteer data may bias indoor-radon statistics toward qualities of volunteers that may not be characteristic of the general population.

A GEOLOGIC MODEL FOR PREDICTING INDOOR-RADON HAZARD ALONG THE WASATCH FRONT

The rating scheme used to assess the potential indoor-radon hazard in the east Sandy and east Provo areas reflects common depositional patterns and physical conditions of geologic units that influence the hazard in both areas. Such patterns and conditions, as well as the techniques used in this study to identify them, are applicable to the identification of areas susceptible to an indoor-radon hazard elsewhere along the Wasatch Front.

In both study areas, geologic units with the highest hazard potential are upper Pleistocene lacustrine sediments related to the Bonneville (transgressive) phase of the Bonneville lake cycle, as well as younger deposits overlying these transgressive units. These units of highest hazard potential are prevalent in elevated benches, locally refered to as the "east bench," along the range front in the eastern part of both study areas. In east Sandy, drainage from Little Cottonwood Canyon has transported material derived principally from Oligocene granitic rocks with a relatively high uranium content to the Little Cottonwood delta (figure 29). Material transported through Big Cottonwood Canyon to the Big Cottonwood delta is derived from a mixed source whose principal component is the Big Cottonwood Formation, relatively deficient in uranium, but whose secondary components include Oligocene granitic rocks and Precambrian metamorphic and sedimentary rocks with higher uranium contents. Houses on well-drained sediments of the east bench near Little Cottonwood Canyon have the highest indoor-radon levels, with an average of 3.8 pCi/L (141 Bq/m^3); 27 percent of these houses have indoor-radon levels above 4 pCi/L (148 Bq/m^3). Sediments below the Provo (regressive) level are not well drained. A significant portion of radon derived from the uranium in these deposits migrates with shallow ground water rather than with soil gas and therefore does not enter houses.

Uranium levels in east Sandy, even on the Big Cottonwood delta, are considerably higher than in east Provo due to differences in source material. In east Provo, uranium-enriched sediment derived from the Mineral Fork Formation and Manning Canyon Shale was mixed with uranium-deficient sediment derived from the Oquirrh Formation. This mixed material was transported through canyon mouths and smaller drainages, and deposited as lacustrine sediments at the Bonneville (transgressive) level of the east bench, and in alluvium on the Provo River delta (figure 30). As in east Sandy, Quaternary geologic units with the highest potential for an indoor-radon hazard are well-drained sediments along the range front, whereas poorly drained units toward the valley interior have a lower hazard potential. Indoor-radon levels in east Provo are also highest on the east bench where they average 2.9 pCi/L (107 Bq/m^3); 17 percent of homes in this area have indoor-radon levels above 4 pCi/L (148 Bq/m^3). In both east Sandy and east Provo uranium content of soils decreases with increasing distance from the range front. This results from increased sediment mixing in valley interiors with material derived from uranium-deficient sources elsewhere in the basin and transported to the study areas

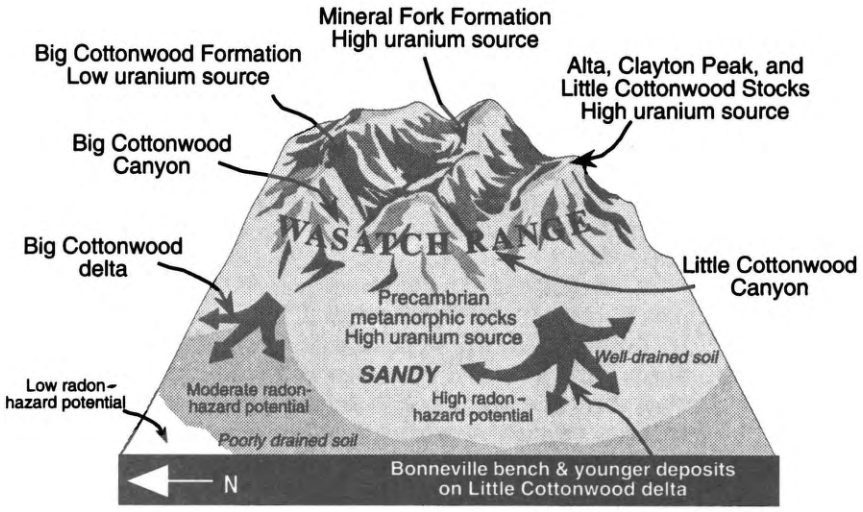

Figure 29. *Sketch of regional geology showing relationship between source and depositional areas, east Sandy. Well-drained, uraniferous deposits with a high radon-hazard potential are derived from rocks in Little Cottonwood Canyon and underlie an elevated bench along the Wasatch Range front. Well-drained but less uraniferous deposits with a moderate radon-hazard potential are derived from rocks in Big Cottonwood Canyon. Poorly drained, uranium-deficient deposits with a low radon-hazard potential are derived from mixed sediment sources and underlie the valley interior.*

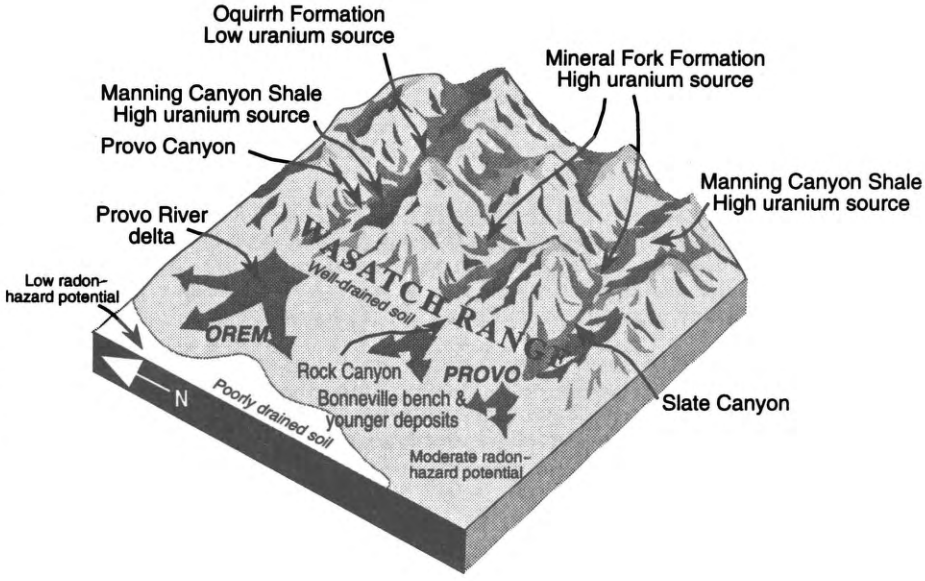

Figure 30. *Sketch of regional geology showing relationship between source and depositional areas, east Provo. Similar depositional patterns in both east Sandy and east Provo resulted in well-drained, uraniferous deposits with the highest radon-hazard potential beneath an elevated bench along the Wasatch Range front. Because uranium levels in east Provo are lower than in east Sandy, bench deposits in east Provo have a moderate radon-hazard potential, rather than high as in east Sandy. As in east Sandy, poorly drained, uranium-deficient deposits in east Provo with a low radon-hazard potential are derived from mixed sediment sources and underlie the valley interior.*

by Lake Bonneville currents.

This combination of distinct source areas with contrasting uranium contents, routes of sediment transport, stratigraphic differentiation in the depositional area, and geomorphic position of well-drained sediments along the range front is a pattern that is likely repeated elsewhere along the Wasatch Front. Techniques used to evaluate potential radon hazard in this study may be applied with equal success in those areas.

CONCLUSIONS

Airborne-radiometric measurements, particularly NURE data, are an effective means of identifying the regional uranium anomalies that are the source of radon in soil gas along the Wasatch Front. These measurements, in conjunction with regional geologic maps, are used to define areas with the potential for generating high concentrations of indoor radon. This is an efficient method for making rapid, quantitative determinations of potential radon-hazard areas.

Ground surveys using gamma-ray spectrometry and alpha scintillometry can rapidly determine the distribution of uranium and soil-gas radon among various geologic units. However, caution is necessary when interpreting soil-gas radon data. Although soil-gas radon levels measured in both the scintillometer (figure 13) and ATD (figure 20) surveys are of the same order of magnitude, details of survey results differ. Reproducibility of both scintillometer and ATD measurements are affected by atmospheric conditions which preclude extrapolation of soil-gas data to other time periods. Reproducibility of ATD measurements is also affected by the duration of the measurement period. Longer measurements give more accurate results. However, the longer a detector is left in the ground, the more likely it will be damaged or lost. In this study a shorter exposure period was used to ensure a high rate of detector recovery. This may have affected the reproducibility of the ATD survey results, but the extent of this effect is unknown. Soil-gas radon data that are not reproducible are useful for indicating relative differences in the level of radon in soil gas, but are not useful for making quantitative estimates of soil-gas radon levels during any period other than the time of measurement. Soil-gas radon data also cannot be used to make quantitative predictions of indoor-radon levels because of the uncertainty introduced by building construction, building maintenance, and occupant lifestyle.

Although uranium and soil-gas radon concentrations are higher in geologic units with higher hazard potential (table 9), the correlation between uranium concentration at the surface measured during the ground survey and soil-gas radon concentration at shallow depth shows considerable scatter (figure 12). The most likely reason for this discrepancy is that the surface material is different from the material at depth that generates the radon-bearing soil gas. This inhomogeneity may have two causes: development and stratigraphy. Because the study areas are largely developed, much of the surface material consists of either imported or disturbed top soil. When the airborne survey was flown in the late 1970s, there was little development and the surface material probably more closely represented the units that generate the radon in the soil gas. Alternately, if the geologic units are naturally stratified, radon measured from soil gas collected at depth may be generated from beds that are not exposed at the surface. In this case the airborne survey, although flown prior to development, measured uranium in beds different from radon-generating units and this difference persists today.

A combination of airborne and ground surveys was used to identify areas with a higher potential for elevated indoor-radon levels in well-drained sediments along the range front in east Sandy, and a similar radon-hazard area was identified along the range front of east Provo with ground studies only. Field work and interpretation were completed in several weeks. Relevant factors of soil-uranium content, soil-gas radon concentration, and ground-water depth were synthesized into a ratings scheme which identified the relative potential for an indoor-radon hazard in buildings in various geologic units. Several other factors affect the indoor-radon hazard, such as weather, construction type, building maintenance, and lifestyle, but characteristics of these factors vary both spatially and temporally and cannot be accurately or efficiently determined for large geographic areas. The general correlation between the indoor-radon-hazard potential, estimated in this study with only geologic criteria, and measured indoor-radon levels support the utility of this rating scheme for predicting the relative potential for indoor-radon hazard in areas without extensive indoor testing. Determining the relative radon-hazard potential for areas underlain by relatively homogenous geologic units allows priorities to be established for indoor testing and hazard reduction in existing construction and demonstrates the need for radon-resistant new construction.

ACKNOWLEDGMENTS

This study was supported by a grant from the EPA, administered by the UDRC, under the SIRG Program. Many persons and organizations provided consent for testing on property under their control; this study would not have been possible without them. The preliminary version of this manuscript (Solomon and others, 1991) was reviewed by Douglas A. Sprinkel, UGS, and the final version was reviewed by Gary Christenson, UGS, and Jonathan G. Price, Nevada Bureau of Mines and Geology; we thank them for their critical comments and helpful suggestions.

REFERENCES CITED

Anderson, L. R., Keaton, J. R., and Bischoff, J. E., 1986a, Liquefaction potential map for Utah County, Utah: Logan, Utah State University, Department of Civil and Environmental Engineering, and Salt Lake City, Dames & Moore Consulting Engineers, 46 p.

Anderson, L. R., Keaton, J. R., Spitzley, J. E., and Allen, A. C., 1986b, Liquefaction potential map for Salt Lake County, Utah: Logan, Utah State University, Department of Civil and Environmental Engineering, and Salt Lake City, Dames & Moore Consulting Engineers, 48 p.

Baker, A. A., 1964, Geology of the Orem quadrangle, Utah: U.S. Geological Survey Map GQ-241, scale 1:24,000.

---1972, Geologic map of the Bridal Veil Falls quadrangle, Utah: U.S. Geological Survey Map GQ-998, scale 1:24,000.

---1973, Geologic map of the Springville quadrangle, Utah: U.S. Geological Survey Map GQ-1103, scale 1:24,000.

Condie, K. C., 1967, Petrology of the late Precambrian tillite(?) association in northern Utah: Geological Society of America Bulletin, v. 78, no. 11, p. 1317-1344.

Crittenden, M. D., Jr., 1976, Stratigraphic and structural setting of the Cottonwood area, Utah, *in* Hill, J. G., editor, Symposium on geology of the Cordilleran hingeline: Denver, Rocky Mountain Association of Geologists, p. 363-379.

Duval, J. S., and Otton, J. K., 1990, Radium distribution and indoor radon in the Pacific Northwest: Geophysical Research Letters, v. 17, no. 6, p. 801-804.

EG&G Geometrics, 1979, Aerial gamma ray and magnetic surveys, Ogden and Salt Lake City quadrangles, Utah: Final Report to the U.S. Department of Energy, v. 1 and 2.

Gundersen, L. C. S., Reimer, G. M., and Agard, S. S., 1988, Correlation between geology, radon in soil gas, and indoor radon in the Reading Prong, *in* Marikos, M. A., and Hansman, R. H., editors, Geologic causes of natural radionuclide anomalies: Missouri Department of Natural Resources, Division of Geology and Land Survey, Special Publication 4, p. 91-102.

Hesselbom, A., 1985, Radon in soil gas - a study of methods and instruments for determining radon concentrations in the ground: Sveriges Geologiska Undersokning (Swedish Geological Survey) Ser. C-803 (in English).

James, L. P., 1979, Geology, ore deposits, and history of the Big Cottonwood mining district, Salt Lake County, Utah: Utah Geological and Mineral Survey Bulletin 114, 98 p.

Machette, M. N., 1989, Preliminary surficial geologic map of the Wasatch fault zone, eastern part of Utah Valley, Utah County and parts of Salt Lake and Juab Counties, Utah: U.S. Geological Survey Miscellaneous Field Studies Map MF-2109, 30 p., scale 1:50,000.

McCammon, R. B., 1980, The statistical treatment of geochemical data, *in* Levinson, A.A., editor, Introduction to exploration geochemistry, 2nd edition: Toronto, Applied Publishing Ltd., p. 835-843.

Muessig, K. W., 1988, Correlation of airborne radiometric data and geologic sources with elevated indoor radon in New Jersey, *in* The 1988 Symposium on Radon and Radon Reduction Technology, preprints: Research Triangle Park, North Carolina, U.S. Environmental Protection Agency, Air and Energy Environmental Research Laboratory, p. V-1.

Nielson, D.L., Linpei, Cui, and Ward, S.H., 1991, Gamma-ray spectrometry and radon emanometry in environmental geophysics, *in* Ward, S.H., editor, Geotechnical and environmental geophysics, v. 1, - review and tutorial: Tulsa, Oklahoma, Society of Exploration Geophysicists, p. 219-250.

Otton, J. K., Schumann, R. R., Owen, D. E., Thurman, Nelson, and Duval, J. S., 1988, Map showing radon potential of rocks and soils in Fairfax County, Virginia: U.S. Geological Survey Miscellaneous Field Studies Map MF-2047, scale 1:48,000.

Oviatt, C.G., Currey, D.R., and Sack, Dorothy, 1992, Radiocarbon chronology of Lake Bonneville, eastern Great Basin, USA: Palaeogeography, Palaeoclimatology, Palaeoecology, v. 99, p. 225-241.

Personius, S. F., and Scott, W. E., 1990, Preliminary surficial geologic map of the Salt Lake City segment and parts of adjacent segments of the Wasatch fault zone, Davis, Salt Lake, and Utah Counties, Utah: U.S. Geological Survey Miscellaneous Field Studies Map MF-2114, scale 1:50,000.

---1992, Surficial geologic map of the Salt Lake City segment and parts of adjacent segments of the Wasatch fault zone, Davis, Salt Lake, and Utah Counties, Utah: U.S. Geological Survey Miscellaneous Investigations Map I-2106, scale 1:50,000.

Reimer, G. M., and Gundersen, L. C. S., 1989, A direct correlation among indoor Rn, soil gas Rn, and geology in the Reading Prong near Boyertown, Pennsylvania: Health Physics, v. 57, no. 1, p. 155-160.

Rogers, J. J. W., 1964, Statistical tests of the homogeneity of the radioactive components of granitic rocks, *in* Makofske, W.J., and Edelstein, M.R., editors, Radon and the environment: Park Ridge, New Jersey, Noyes Publications, p. 51-62.

Rogers, V. C., and Nielson, K. K., 1990, Benchmark and application of the RAETRAD model, *in* The 1990 International Symposium on Radon and Radon Reduction Technology, v. III, preprints: Research Triangle Park, North Carolina, U.S. Environmental Protection Agency, Air and Energy Environmental Research Laboratory, EPA/600/9-90/005c, p. VI-1.

Schery, W. R., Gaeddert, D. H., and Wilkening, M. H., 1984, Factors affecting exhalation of radon from a gravelly sandy loam: Journal of Geophysical Research, v. 89, p. 7299-7309.

Sextro, Richard, 1988, Radon in dwellings, *in* Makofske, W.J., and Edelstein, M.R., editors, Radon and the environment: Park Ridge, New Jersey, Noyes Publications, p. 71-82.

Solomon, B. J., Black, B. D., Nielson, D, L., and Cui, Linpei, 1991, Identification of radon-hazard areas along the Wasatch Front, Utah, using geologic techniques, *in* McCalpin, J. P., editor, Proceedings of the 27th Symposium on Engineering Geology and Geotechnical Engineering: Logan, Utah State University, p. 40-1 - 40-16.

Sprinkel, D. A., 1987 (revised 1988), The potential radon hazard map, Utah: Utah Geological and Mineral Survey Open-File Report 108, 4 p., scale 1:1,000,000.

Sprinkel, D. A., and Solomon, B. J., 1990, Radon hazards in Utah: Utah Geological and Mineral Survey Circular 81, 24 p.

Stranden, Erling, 1984, Thoron (^{220}Rn) daughter to radon (^{222}Rn) daughter ratios in thorium-rich areas: Health Physics, v. 47, no. 5, p. 784-785.

Swenson, J. L., Jr., Archer, W. M., Donaldson, K. M., Shiozaki, J. J., Broderick, J. H., and Woodward, Lowell, 1972, Soil survey of Utah County, Utah - central part: U.S. Department of Agriculture Soil Conservation Service in cooperation with Utah Agricultural Experiment Station, 161 p.

Tanner, A. B., 1964, Radon migration in the ground, a review, *in* Adams, J. A. S., and Lowder, W. M., editors, The natural radiation environment: University of Chicago Press, p. 161-190.

---1980, Radon migration in the ground - a supplementary review, *in* Gesell, T. F., and Lowder, W. M., editors, Natural Radiation Environment III: Symposium Proceedings, Houston, v. 1, U.S. Department of Energy Report CONF-780422, National Technical Information Service, p. 5-56.

U.S. Environmental Protection Agency, 1989, Radon measurement in schools, an interim report: U.S. Environmental Protection Agency Report EPA-520/1-89-010, 17 p.

U.S. Environmental Protection Agency, U.S. Department of Health and Human Services, and U.S. Public Health Service, 1992, A citizen's guide to radon (second edition): U.S. Environmental Protection Agency, Office of Air and Radiation Report 402-K92-001, 15 p.

U.S. Soil Conservation Service, 1975, Soil taxonomy: Washington, D.C., U.S. Department of Agriculture Handbook No. 436, p. 469-474.

Washington, J. W., and Rose, A. W., 1992, Temporal variability of radon concentration in the interstitial gas of soils in Pennsylvania: Journal of Geophysical Research, v. 97, no. B6, p. 9145-9159.

Witcher, J. C., and Shoenmackers, R., 1990, Time-integrated radon soil-gas surveys in geothermal exploration in the southern Rio Grande rift, New Mexico: New Mexico Research and Development Institute Report, 175 p.

Woodward, Lowell, Harvey, J. L., Donaldson, K. M., Shiozaki, J. J., Leishman, G. W., and Broderick, J. H., 1974, Soil survey of Salt Lake area, Utah: U.S. Department of Agriculture Soil Conservation Service in cooperation with Utah Agricultural Experiment Station, 132 p.

APPENDIX

Ground-Survey Data (Except Soil-ATD Measurements)

Table A-1

Indoor-radon measurements, east Sandy, collected for both this study and the statewide survey (Sprinkel and Solomon, 1990). Measurements are grouped by geologic unit, and are sorted within each unit in descending order by indoor-radon concentration. See table 1 for explanation of geologic units. Specific locations are withheld to protect the confidentiality of survey participants.

Sample Number	Geologic Unit	Indoor Radon (pCi/L)	Ground-Water Depth (ft)	Zip Code
483484	af2	3.2	<10	84020
842197	af2	2.8	>50	84092
483544	af2	2.7	<10	84020
839709	af2	2.2	>50	84092
483524	af2	1.7	>50	84092
842166	al1	1.1	<10	84093
842213	al2	26.2	10-30	84092
483482	al2	6.8	10-30	84093
842193	al2	5.1	10-30	84093
839786	al2	4.3	10-30	84093
839743	al2	2.5	<10	84093
483400	alp bcc	3.8	10-30	84121
483676	alp bcc	3.3	10-30	84121
483290	alp bcc	1.5	10-30	84121
839661	alp bcc	1.5	10-30	84121
1679401	alp lcc	13.7	>50	84093
483231	alp lcc	12.7	10-30	84093
1679414	alp lcc	11.6	>50	84093
839707	alp lcc	11.3	>50	84093
842241	alp lcc	10.7	>50	84093
483242	alp lcc	10.0	>50	84092
839653	alp lcc	9.7	>50	84093
839752	alp lcc	9.0	>50	84092
839694	alp lcc	8.8	>50	84093
839712	alp lcc	8.7	>50	84093
483176	alp lcc	8.5	>50	84093
842190	alp lcc	7.2	>50	84092
842207	alp lcc	7.0	10-30	84093
839788	alp lcc	6.8	>50	84093
842230	alp lcc	6.8	10-30	84092
839681	alp lcc	6.3	>50	84092
839740	alp lcc	4.5	>50	84093
839698	alp lcc	4.5	10-30	84093
842224	alp lcc	4.4	>50	84093
839732	alp lcc	4.4	30-50	84093
839679	alp lcc	4.3	>50	84093
842254	alp lcc	4.3	>50	84093
842199	alp lcc	4.3	10-30	84093
483507	alp lcc	4.1	30-50	84093
842177	alp lcc	3.9	>50	84093
842163	alp lcc	3.9	30-50	84093
842211	alp lcc	3.7	>50	84093
483160	alp lcc	3.7	>50	84092
839685	alp lcc	3.5	>50	84093
483167	alp lcc	3.4	>50	84093
839738	alp lcc	3.3	>50	84093
842212	alp lcc	3.3	>50	84093
484575	alp lcc	3.2	>50	84092
839666	alp lcc	3.2	>50	84092
842172	alp lcc	3.1	>50	84093
839777	alp lcc	2.9	>50	84092
842235	alp lcc	2.8	30-50	84093
839717	alp lcc	2.7	>50	84093
842178	alp lcc	2.7	>50	84093
842192	alp lcc	2.7	>50	84093
839734	alp lcc	2.6	>50	84093
839736	alp lcc	2.6	>50	84093
842240	alp lcc	2.6	30-50	84093
839733	alp lcc	2.6	10-30	84093
842176	alp lcc	2.5	30-50	84094
839702	alp lcc	2.5	30-50	84093
483515	alp lcc	2.4	>50	84093
839660	alp lcc	2.4	>50	84093
483747	alp lcc	2.4	>50	84092
839719	alp lcc	2.3	>50	84093
839655	alp lcc	2.3	>50	84092
842204	alp lcc	2.2	>50	84093
839701	alp lcc	2.2	>50	84092
839676	alp lcc	2.2	30-50	84093
839703	alp lcc	2.2	10-30	84093
1679396	alp lcc	2.1	>50	84093
483766	alp lcc	2.1	30-50	84094
839735	alp lcc	2.0	>50	84093
839720	alp lcc	2.0	>50	84092
839671	alp lcc	1.9	>50	84093

***Table A-1** (continued)*

Sample Number	Geologic Unit	Indoor Radon (pCi/L)	Ground-Water Depth (ft)	Zip Code
839758	alp lcc	1.9	10-30	84093
842169	alp lcc	1.7	>50	84093
839784	alp lcc	1.7	>50	84092
842206	alp lcc	1.6	>50	84093
842242	alp lcc	1.5	>50	84093
842195	alp lcc	1.5	>50	84092
842167	alp lcc	1.5	30-50	84093
839687	alp lcc	1.5	10-30	84093
839691	alp lcc	1.5	10-30	84092
839787	alp lcc	1.4	>50	84093
842179	alp lcc	1.4	>50	84093
842174	alp lcc	1.4	>50	84092
839663	alp lcc	1.4	30-50	84093
483252	alp lcc	1.3	30-50	84093
839699	alp lcc	1.3	30-50	84093
839706	alp lcc	1.3	30-50	84093
839730	alp lcc	1.2	10-30	84093
839690	alp lcc	1.1	>50	84093
839727	alp lcc	1.1	10-30	84121
839665	alp lcc	0.9	30-50	84093
842252	alp lcc	0.8	10-30	84093
839680	alp lcc	0.6	>50	84093
839662	alp lcc	0.6	>50	84092
839723	alp lcc	0.5	>50	84092
483799	ca bcc	2.2	10-30	84121
839700	ca lcc	4.4	>50	84121
839670	ca lcc	3.2	>50	84093
839757	ca lcc	2.7	>50	84092
839675	ca lcc	2.3	>50	84092
839725	ca lcc	1.8	>50	84092
839678	ca lcc	1.2	>50	84092
839682	ca lcc	1.2	>50	84092
839789	ca lcc	1.0	>50	84093
842248	ca lcc	0.7	>50	84092
839692	cd1	1.9	>50	84121
842198	cd1	1.3	>50	84121
483181	chs	2.4	>50	84121
1679391	es	3.4	>50	84092
839741	es	3.1	>50	84092
483760	es	3.0	30-50	84070
839739	es	2.9	>50	84092
483266	es	2.3	>50	84092
842194	es	2.3	>50	84092
483759	es	2.3	30-50	84121
483152	es	2.0	>50	84092
842188	es	2.0	>50	84092
483336	es	1.8	>50	84092
839704	es	1.8	>50	84092
839724	es	1.7	>50	84092
842261	es	1.7	>50	84092
1679410	es	1.7	>50	84092
842234	es	1.5	>50	84092
839659	es	1.4	>50	84092
839767	es	1.4	>50	84092
634621	es	1.3	10-30	84121
483651	es	1.2	10-30	84070
483549	es	1.1	>50	84092
839656	es	1.1	>50	84092
483518	es	1.1	30-50	84094
842164	es	1.0	>50	84092
842249	es	1.0	>50	84092
842162	es	0.9	>50	84092
839674	es	0.8	>50	84092
839759	es	0.8	>50	84092
842238	es	0.7	>50	84092
483684	f	2.2	>50	84121
839726	gbco	2.7	>50	84092
842214	gbct	6.1	>50	84092
483580	lbg bcc	1.1	10-30	84121
1679412	lbg bcc	0.5	10-30	84121
483803	lbg lcc	26.2	>50	84092
839658	lbg lcc	9.1	>50	84092
839794	lbg lcc	4.8	>50	84093
483547	lbg lcc	4.4	>50	84121
839731	lbg lcc	3.1	>50	84092
842210	lbg lcc	2.3	>50	84092

***Table A-1** (continued)*

Sample Number	Geologic Unit	Indoor Radon (pCi/L)	Ground-Water Depth (ft)	Zip Code
842220	lbg lcc	1.9	10-30	84121
839772	lbg lcc	1.8	>50	84092
842200	lbg lcc	1.6	>50	84092
842170	lbg lcc	1.4	30-50	84121
839718	lbg lcc	1.3	>50	84092
842202	lbg lcc	1.0	>50	84092
842250	lbg lcc	1.0	>50	84092
839797	lbg lcc	1.0	30-50	84121
842180	lbg lcc	0.9	>50	84092
839760	lbg lcc	0.3	>50	84092
483608	lbpm	0.8	<10	84020
483640	lpd	1.3	10-30	84094
483806	lpd	0.9	10-30	84092
483241	lpg	8.8	>50	84092
483177	lpg	6.2	>50	84092
842236	lpg	4.6	30-50	84092
1679393	lpg	4.0	>50	84092
483386	lpg	3.7	>50	84092
1679381	lpg	3.7	>50	84092
839705	lpg	3.5	>50	84092
483538	lpg	3.0	>50	84070
839654	lpg	2.8	>50	84092
839721	lpg	2.8	>50	84092
842221	lpg	2.7	>50	84092
839729	lpg	2.6	>50	84092
839696	lpg	2.5	>50	84092
842203	lpg	2.5	>50	84092
842233	lpg	2.4	>50	84092
483480	lpg	2.2	>50	84092
839744	lpg	2.2	>50	84092
842251	lpg	2.2	>50	84092
483247	lpg	2.1	>50	84092
839693	lpg	1.8	>50	84092
842175	lpg	1.8	>50	84092
839668	lpg	1.8	>50	84092
839770	lpg	1.7	>50	84092
483270	lpg	1.7	10-30	84121
483564	lpg	1.6	30-50	84092
483485	lpg	1.6	10-30	84070
842165	lpg	1.5	>50	84092
842227	lpg	1.4	>50	84092
839722	lpg	1.3	>50	84092
839776	lpg	1.3	>50	84092
842253	lpg	1.2	>50	84093
483599	lpg	1.2	10-30	84121
842255	lpg	1.1	>50	84092
483584	lpg	0.9	30-50	84094
634596	lpg	0.9	30-50	84070
483519	lpg	0.9	10-30	84121
483471	lpg	0.8	10-30	84070
842181	lpg	0.6	>50	84092
483722	lpg	0.6	>50	84070
484542	lpg	0.5	>50	84092
842182	lpg	0.5	>50	84092
483741	lpg	0.5	30-50	84070

Table A-2

Indoor-radon measurements, east Provo, collected for both this study and the statewide survey (Sprinkel and Solomon, 1990). Measurements are grouped by geologic unit, and are sorted within each unit in descending order by indoor-radon concentration. See table 2 for explanation of geologic units. Specific locations are withheld to protect the confidentiality of survey participants.

Sample Number	Geologic Unit	Indoor Radon (pCi/L)	Ground-Water Depth (ft)	Zip Code
483390	af2	8.2	10-30	84604
483300	af4	0.9	>50	84604
634598	afb	1.4	>50	84604
842189	afp	8.1	10-50	84604
842205	afp	3.1	<10	84606
839802	afp	1.6	<10	84606
839768	afp	1.5	<10	84606
842245	afp	1.1	<10	84606
842229	afp	1.0	<10	84606
839710	afp	1.0	<10	84601
842215	afp	0.8	<10	84606
842228	afp	0.7	<10	84606
483743	afp	0.5	>50	84604
483348	afy	10.2	10-50	84604
839684	afy	7.8	>50	84604
483508	afy	7.0	>50	84604
842185	afy	6.5	>50	84604
483388	afy	5.4	<10	84601
839801	afy	4.1	10-50	84604
842209	afy	3.9	>50	84604
839711	afy	3.2	10-50	84604
483829	afy	3.1	>50	84604
839792	afy	3.0	>50	84604
839779	afy	2.4	>50	84606
839754	afy	2.4	>50	84604
842243	afy	2.2	>50	84604
483375	afy	2.2	<10	84601
839715	afy	2.1	>50	84604
839764	afy	2.1	>50	84604
483341	afy	2.1	>50	84601
842244	afy	2.0	>50	84604
839673	afy	2.0	<10	84606
842187	afy	1.6	<10	84606
839756	afy	1.6	10-50	84606
483800	afy	1.5	>50	84601
842168	afy	1.5	10-50	84604
839778	afy	1.4	>50	84604
839785	afy	1.4	10-50	84604
634601	afy	1.3	>50	84604
483268	afy	1.3	<10	84601
839781	afy	1.3	10-50	84604
483573	afy	1.2	>50	84604
842225	afy	1.2	<10	84606
839753	afy	0.8	>50	84604
483808	afy	0.7	<10	84601
483198	afy	0.7	10-50	84601
839790	afy	0.6	10-50	84604
483764	al2	6.5	<10	84604
483820	al2	1.0	<10	84604
483826	alp	6.3	10-50	84604
483744	alp	4.6	10-50	84058
483314	alp	4.0	>50	84057
483516	alp	3.9	>50	84058
483802	alp	3.9	10-50	84604
483309	alp	3.7	>50	84604
483394	alp	3.7	>50	84057
634591	alp	3.7	>50	84057
483779	alp	3.5	10-50	84058
483605	alp	3.4	10-50	84057
483191	alp	3.3	>50	84057
483828	alp	3.3	10-50	84058
483603	alp	2.9	>50	84057
483387	alp	2.8	>50	84057
483378	alp	2.7	10-50	84058
483812	alp	2.3	10-50	84058
483624	alp	2.2	>50	84057
483173	alp	2.0	<10	84058
634629	alp	1.8	10-50	84057
483202	alp	1.7	<10	84058
483742	alp	1.7	10-50	84057
483207	alp	1.6	>50	84057
483491	alp	1.4	10-50	84058
483269	alp	1.3	10-50	84058
634595	alp	1.3	10-50	84057
483279	alp	1.1	10-50	84058

Table A-2 (continued)

Sample Number	Geologic Unit	Indoor Radon (pCi/L)	Ground-Water Depth (ft)	Zip Code
483398	alp	1.1	10-50	84057
483287	alp	1.0	>50	84604
483226	alp	1.0	10-50	84058
634580	alp	0.6	>50	84057
483791	alp	0.2	10-50	84058
483733	clso	3.4	>50	84604
483537	es	3.8	10-50	84057
483704	es	2.7	10-50	84057
483735	es	2.0	10-50	84057
483512	es	0.9	10-50	84058
483715	es	0.6	10-50	84057
839799	lbg	3.7	>50	84604
483805	lbg	2.7	>50	84604
483711	lbg	2.6	>50	84604
842260	lbg	2.1	>50	84604
483505	lbm	13.6	10-50	84604
842246	lbm	9.1	>50	84604
483525	lbm	8.7	10-50	84604
839800	lbm	8.4	10-50	84604
842237	lbm	5.5	>50	84604
842183	lbm	4.1	>50	84604
839686	lbm	4.0	10-50	84604
842201	lbm	3.9	>50	84604
483748	lbm	3.3	>50	84057
839771	lbm	3.2	>50	84604
839689	lbm	2.9	>50	84601
839714	lbm	2.9	10-50	84604
483271	lbm	2.9	10-50	84604
839762	lbm	2.7	>50	84604
483310	lbm	2.6	10-50	84604
839765	lbm	2.2	10-50	84604
634599	lbm	2.1	10-50	84604
839742	lbm	1.8	10-50	84604
839755	lbm	1.4	10-50	84604
839793	lbm	1.1	>50	84604
839796	lbm	1.1	10-50	84604
483789	lbm	0.9	>50	84604
483331	lbm	0.7	>50	84604
483393	lbm	0.7	>50	84604
483807	lbs	9.9	>50	84604
483723	lbs	2.1	>50	84604
483776	lbs	2.0	>50	84604
839783	lbs	2.0	>50	84604
839782	lbs	1.9	>50	84604
1679375	lbs	1.9	>50	84604
842259	lbs	1.7	>50	84604
842186	lbs	1.6	>50	84604
842196	lbs	1.0	>50	84604
483453	lbs	0.9	>50	84604
842171	lbs	0.9	>50	84604
1679407	lbs	0.9	>50	84604
483289	lbs	0.8	>50	84604
483389	lbs	0.8	>50	84604
483817	lbs	0.8	>50	84604
839795	lbs	0.7	>50	84606
839774	lbs	0.7	>50	84604
839761	lpd	2.3	10-50	84604
483550	lpd	2.2	10-50	84057
839697	lpd	1.7	10-50	84604
483343	lpd	1.5	10-50	84058
483734	lpd	0.6	10-50	84058
483452	lpg	2.5	10-50	84604
483361	lpg	2.4	10-50	84604
483714	lpg	2.2	10-50	84058
483781	lpg	2.2	10-50	84058
483359	lpg	1.5	10-50	84058
483757	lpg	1.5	10-50	84058
483513	lpg	1.4	10-50	84057
483285	lpg	1.3	10-50	84058
839769	lpm	1.9	<10	84606
842247	lpm	1.6	<10	84606
1679399	lpm	1.3	<10	84606
839798	lpm	0.8	<10	84606
839775	lpm	0.5	<10	84606
483493	lps	1.7	<10	84058
839716	lps	1.7	10-50	84606
483662	lps	0.8	10-50	84058

Table A-3.

Ground-survey data, east Sandy, exclusive of indoor- and soil-ATD measurements. Measurements are grouped by geologic unit, and are sorted within each unit in descending order by eU concentration. See table 1 for explanation of geologic units.

Sample Number	Geologic Unit	Total Counts (ppm)	eK (%)	eU (ppm)	eTh (ppm)	eU/eTh	Soil Gas Rn (pCi/L)	Ground-Water Depth (ft)
S-008	af1	19.0	2.6	4.2	14.3	0.29	–	>50
S-041	af2	27.3	3.4	6.0	19.2	0.31	–	>50
S-116	af2	16.5	1.6	5.2	12.3	0.42	–	10-30
S-096	af2	16.8	1.8	4.0	14.1	0.28	–	>50
S-005	af2	18.4	2.4	3.6	17.1	0.21	120	<10
S-010	af2	15.8	2.6	2.9	10.3	0.28	–	>50
S-007	af2	18.8	2.6	2.3	20.6	0.11	–	30-50
S-112	al1	25.5	2.6	9.0	14.2	0.63	246	<10
S-102	al1	24.6	2.7	8.5	11.4	0.75	482	<10
S-083	al1	24.7	3.1	7.9	12.5	0.63	–	<10
S-130	al1	21.9	2.1	6.4	16.2	0.40	–	10-30
S-104	al1	21.8	2.2	6.2	16.5	0.38	–	<10
S-004	al1	19.9	2.8	2.9	19.0	0.15	82	<10
S-118	al2	15.4	1.7	3.7	11.6	0.32	–	10-30
S-131	alp bcc	16.7	1.6	5.5	11.2	0.49	–	10-30
S-125	alp bcc	12.2	1.6	2.6	10.0	0.26	–	10-30
S-064	alp lcc	26.3	2.8	8.7	15.3	0.57	516	>50
S-084	alp lcc	20.8	2.2	8.7	9.7	0.90	143	30-50
S-037	alp lcc	28.0	3.0	8.7	16.6	0.52	–	>50
S-073	alp lcc	23.4	2.3	8.4	12.1	0.69	861	>50
S-120	alp lcc	25.1	2.7	8.4	16.4	0.51	314	30-50
S-127	alp lcc	26.5	2.9	8.2	15.6	0.53	–	10-30
S-122	alp lcc	23.5	2.2	8.2	13.9	0.59	–	10-30
S-045	alp lcc	25.4	2.5	7.9	16.1	0.49	311	>50
S-038	alp lcc	27.8	3.2	7.9	17.8	0.44	279	>50
S-075	alp lcc	25.3	2.8	7.5	14.3	0.52	1021	10-30
S-105	alp lcc	25.0	2.8	7.5	18.8	0.40	–	<10
S-039	alp lcc	24.2	2.8	7.3	12.6	0.58	368	>50
S-126	alp lcc	25.1	2.8	7.3	12.0	0.61	–	10-30
S-063	alp lcc	25.1	2.7	7.2	14.8	0.49	2398	>50
S-047	alp lcc	24.0	2.5	7.1	14.6	0.49	402	>50
S-065	alp lcc	24.8	2.9	7.1	16.4	0.43	–	>50
S-046	alp lcc	21.0	2.2	7.0	11.6	0.60	1138	>50
S-040	alp lcc	26.9	3.1	7.0	16.9	0.41	–	>50
S-061	alp lcc	22.3	2.3	6.9	12.5	0.55	548	>50
S-062	alp lcc	21.4	2.2	6.8	9.4	0.72	95	30-50
S-076	alp lcc	24.8	2.5	6.8	15.8	0.43	–	>50

***Table A-3** (continued)*

Sample Number	Geologic Unit	Total Counts (ppm)	eK (%)	eU (ppm)	eTh (ppm)	eU/eTh	Soil Gas Rn (pCi/L)	Ground-Water Depth (ft)
S-072	alp lcc	24.1	2.7	6.5	13.7	0.47	503	30-50
S-129	alp lcc	23.9	2.7	6.5	15.6	0.42	–	10-30
S-092	alp lcc	19.8	2.2	6.0	12.7	0.47	–	>50
S-074	alp lcc	17.5	1.8	5.8	9.0	0.64	290	>50
S-081	alp lcc	19.3	2.3	5.4	11.4	0.47	–	>50
S-066	alp lcc	21.8	2.5	5.3	15.4	0.34	–	>50
S-068	alp lcc	16.0	1.6	5.2	10.5	0.50	–	>50
S-067	alp lcc	22.3	3.1	5.0	13.2	0.38	–	>50
S-069	alp lcc	21.1	2.9	4.9	15.7	0.31	–	>50
S-052	alp lcc	22.9	2.7	4.3	17.8	0.24	–	>50
S-014	alp lcc	13.5	1.6	3.2	11.5	0.28	1069	>50
S-110	ca bcc	26.1	2.6	8.4	17.2	0.49	466	10-30
S-117	ca bcc	18.9	2.0	5.9	15.2	0.39	–	<10
S-124	ca bcc	14.0	1.7	4.1	10.6	0.39	283	10-30
S-119	ca bcc	14.1	1.8	3.6	10.4	0.35	–	>50
S-113	ca lcc	24.3	2.5	7.7	14.8	0.52	–	30-50
S-115	ca lcc	21.0	2.0	7.2	14.5	0.50	–	>50
S-128	ca lcc	21.4	2.4	6.7	12.7	0.53	–	10-30
S-056	ca lcc	16.8	2.4	3.8	12.9	0.29	–	>50
S-095	chs	23.7	3.4	5.7	17.5	0.33	–	>50
S-094	chs	19.2	2.3	5.6	12.2	0.46	–	>50
S-082	es	24.0	2.6	8.2	12.8	0.64	–	<10
S-044	es	26.2	2.9	6.4	16.2	0.40	–	>50
S-048	es	20.0	2.5	5.4	10.7	0.50	–	>50
S-078	es	21.0	2.7	5.3	10.8	0.49	–	>50
S-049	es	19.9	2.4	4.7	11.6	0.41	–	>50
S-077	es	19.5	2.6	4.5	9.8	0.46	–	>50
S-080	es	17.9	2.1	3.8	13.0	0.29	–	>50
S-054	es	15.6	2.3	2.7	12.7	0.21	–	>50
S-089	gbco	25.6	2.9	7.4	13.7	0.54	–	>50
S-090	gbco	24.2	2.5	6.6	16.8	0.39	–	>50
S-091	gbct	25.5	3.3	6.3	17.0	0.37	–	>50
S-093	gbct	20.6	2.4	5.1	14.8	0.34	–	>50
S-003	laly	11.9	1.4	3.3	9.3	0.35	138	<10
S-002	laly	13.3	1.8	3.0	10.5	0.29	905	<10
S-109	lbg bcc	24.2	2.5	8.6	12.0	0.72	265	10-30
S-108	lbg bcc	17.5	1.7	5.6	10.7	0.52	327	30-50

***Table A-3** (continued)*

Sample Number	Geologic Unit	Total Counts (ppm)	eK (%)	eU (ppm)	eTh (ppm)	eU/eTh	Soil Gas Rn (pCi/L)	Ground-Water Depth (ft)
S-042	lbg lcc	23.2	2.5	7.9	10.9	0.72	126	>50
S-114	lbg lcc	22.2	2.2	7.2	14.6	0.49	–	30-50
S-043	lbg lcc	19.6	2.1	6.6	9.9	0.67	1082	>50
S-050	lbg lcc	23.4	2.8	5.4	15.9	0.34	–	>50
S-051	lbg lcc	22.6	2.6	5.3	15.8	0.34	–	>50
S-029	lbg lcc	21.3	2.6	5.0	12.9	0.39	404	>50
S-079	lbg lcc	18.6	2.3	4.9	13.8	0.36	–	>50
S-106	lbg lcc	16.5	1.8	4.8	11.0	0.44	–	10-30
S-055	lbg lcc	17.0	2.3	4.3	11.9	0.36	–	>50
S-018	lbg lcc	17.3	2.5	3.4	13.3	0.26	203	>50
S-053	lbg lcc	20.2	2.6	3.4	16.9	0.20	–	>50
S-011	lbg lcc	15.5	2.3	3.2	13.0	0.25	–	>50
S-009	lbg lcc	17.5	2.9	2.7	15.6	0.17	–	>50
S-013	lbg lcc	11.3	1.6	2.2	9.8	0.22	912	>50
S-012	lbg lcc	11.3	1.4	1.8	10.6	0.17	1198	>50
S-087	lbpm	19.3	2.1	5.1	11.2	0.46	580	10-30
S-001	lbpm	15.0	2.0	2.4	14.0	0.17	309	<10
S-121	lpd	26.1	2.4	9.0	14.1	0.64	–	10-30
S-103	lpd	26.2	3.0	8.8	15.0	0.59	–	10-30
S-111	lpd	23.8	2.2	8.6	13.2	0.65	223	10-30
S-071	lpd	21.8	2.0	7.3	11.5	0.63	613	10-30
S-059	lpd	28.3	3.2	7.3	14.6	0.50	–	>50
S-100	lpd	22.5	2.7	6.6	8.7	0.76	110	10-30
S-123	lpd	11.8	1.4	2.4	10.2	0.24	–	10-30
S-097	lpg	25.5	2.2	10.6	13.5	0.79	730	10-30
S-035	lpg	27.2	3.2	8.0	13.3	0.60	–	30-50
S-026	lpg	21.8	2.1	7.5	13.7	0.55	72	30-50
S-036	lpg	25.5	3.1	7.0	12.6	0.56	–	>50
S-101	lpg	24.5	2.7	6.8	16.9	0.40	309	10-30
S-028	lpg	27.4	3.2	6.4	17.5	0.37	749	>50
S-025	lpg	23.8	2.6	6.4	13.7	0.47	371	>50
S-030	lpg	24.6	3.4	6.3	8.3	0.76	–	30-50
S-086	lpg	22.5	2.5	6.2	12.7	0.49	711	<10
S-060	lpg	22.5	2.4	6.2	13.7	0.45	564	30-50
S-088	lpg	20.6	2.0	6.1	13.4	0.46	73	10-30
S-099	lpg	19.7	2.4	6.0	8.6	0.70	270	10-30
S-085	lpg	20.4	2.6	5.6	12.0	0.47	702	10-30
S-027	lpg	22.4	2.7	5.6	13.1	0.43	624	>50

***Table A-3** (continued)*

Sample Number	Geologic Unit	Total Counts (ppm)	eK (%)	eU (ppm)	eTh (ppm)	eU/eTh	Soil Gas Rn (pCi/L)	Ground-Water Depth (ft)
S-032	lpg	21.2	2.8	5.6	9.1	0.62	–	30-50
S-034	lpg	21.0	2.6	5.5	12.3	0.45	–	>50
S-031	lpg	25.7	3.8	5.0	11.2	0.45	–	30-50
S-107	lpg	16.0	1.8	4.9	10.8	0.45	–	10-30
S-070	lpg	15.8	1.8	4.1	12.2	0.34	–	>50
S-098	lpg	19.2	2.2	4.0	14.4	0.28	1194	10-30
S-033	lpg	22.0	3.4	4.0	8.8	0.45	–	10-30
S-015	lpg	17.8	2.4	3.7	14.1	0.26	–	30-50
S-017	lpg	12.9	1.7	3.4	9.6	0.35	114	30-50
S-023	lpg	17.5	2.2	3.3	16.5	0.20	–	30-50
S-022	lpg	12.8	1.6	3.2	7.9	0.41	968	>50
S-021	lpg	13.5	1.9	2.4	9.8	0.24	1434	30-50
S-057	lpg	15.1	2.0	2.3	13.3	0.17	–	>50
S-006	lpg	11.8	1.7	2.2	8.5	0.26	456	>50
S-024	lpg	17.8	2.7	2.2	16.8	0.13	–	30-50
S-016	lpg	13.1	1.9	1.9	8.6	0.22	354	30-50
S-058	lpg	16.2	2.5	1.9	13.1	0.15	–	>50
S-019	lpg	11.0	1.8	1.5	8.0	0.19	220	>50
S-020	lpg	13.8	1.9	1.2	12.8	0.09	332	>50

Table A-4

Ground-survey data, east Provo, exclusive of indoor- and soil-ATD measurements. Measurements are grouped by geologic unit, and are sorted within each unit in descending order by eU concentration. See table 2 for explanation of geologic units.

Sample Number	Geologic Unit	Total Counts (ppm)	eK (%)	eU (ppm)	eTh (ppm)	eU/eTh	Soil Gas Rn (pCi/L)	Ground-Water Depth (ft)
P-037	af2	8.8	1.1	3.4	5.3	0.64	281	10-30
P-046	af2	11.8	1.3	3.3	6.7	0.49	–	10-50
P-011	af2	8.8	1.1	2.7	5.9	0.46	1454	<10
P-091	af2	7.8	0.9	2.7	6.9	0.39	1264	<10
P-047	af2	9.1	1.2	2.5	5.4	0.46	–	10-50
P-061	af2	9.9	1.3	1.9	8.6	0.22	354	10-30
P-062	af2	10.5	1.3	1.9	9.7	0.20	224	10-30
P-010	af2	7.1	1.0	1.8	4.8	0.38	497	<10
P-044	afp	10.5	1.2	3.6	6.5	0.55	65	<10
P-016	afp	9.8	1.1	3.3	6.1	0.54	–	10-50
P-033	afp	10.2	1.2	2.9	6.3	0.46	468	<10
P-041	afp	9.2	1.0	2.9	7.5	0.39	180	<10
P-038	afp	9.5	1.3	2.3	5.2	0.44	253	<10
P-036	afp	8.2	1.2	1.5	6.0	0.25	202	<10
P-056	afy	14.1	1.7	4.6	9.4	0.49	–	>50
P-034	afy	11.2	1.3	4.3	7.0	0.61	1405	<10
P-067	afy	11.2	1.4	4.0	7.3	0.55	527	>50
P-021	afy	9.6	1.1	3.3	5.7	0.58	683	10-50
P-068	afy	12.2	1.6	3.3	8.9	0.37	215	>50
P-012	afy	7.8	0.7	3.0	6.4	0.47	889	>50
P-019	afy	9.3	0.8	2.9	7.6	0.38	87	10-50
P-039	afy	10.9	1.3	2.9	6.5	0.45	–	<10
P-054	afy	8.8	1.1	2.8	4.1	0.68	–	10-50
P-089	afy	10.8	1.8	2.7	6.5	0.42	–	>50
P-030	afy	7.1	1.0	2.6	3.8	0.68	–	>50
P-051	afy	8.8	1.1	2.6	6.4	0.41	–	<10
P-035	afy	7.9	0.9	2.4	5.9	0.41	214	10-50
P-084	afy	6.3	0.6	2.4	3.9	0.62	–	>50
P-020	afy	7.5	0.8	2.3	7.0	0.33	716	10-50
P-023	afy	8.8	1.2	2.3	5.2	0.44	290	<10
P-083	afy	6.9	0.9	2.0	7.0	0.29	–	>50
P-007	afy	8.8	1.4	1.9	6.6	0.29	325	10-50
P-005	afy	8.1	0.9	1.8	5.9	0.31	336	10-50
P-001	al1	12.7	1.4	4.0	8.1	0.49	187	<10
P-092	al1	6.7	0.7	1.9	5.2	0.37	–	<10
P-052	al2	10.1	1.2	3.9	7.1	0.55	519	<10
P-002	al2	11.0	1.3	2.8	7.5	0.37	–	<10

***Table A-4** (continued)*

Sample Number	Geologic Unit	Total Counts (ppm)	eK (%)	eU (ppm)	eTh (ppm)	eU/eTh	Soil Gas Rn (pCi/L)	Ground-Water Depth (ft)
P-048	al2	9.5	1.2	2.6	7.5	0.35	–	<10
P-065	al2	8.0	1.1	2.4	5.5	0.44	–	<10
P-050	al2	8.4	1.0	2.0	8.9	0.22	–	<10
P-099	al2	6.6	1.0	1.9	3.5	0.54	407	<10
P-013	al2	6.8	1.0	1.9	4.1	0.46	–	<10
P-093	al2	7.6	0.9	1.7	5.9	0.29	887	<10
P-079	alp	9.1	1.0	3.3	7.5	0.44	630	>50
P-058	alp	10.6	1.2	3.3	8.2	0.40	86	>50
P-070	alp	11.2	1.6	3.2	7.5	0.43	318	>50
P-026	alp	10.0	1.2	3.2	6.5	0.49	–	>50
P-073	alp	6.7	0.8	2.8	4.2	0.67	–	<10
P-059	alp	5.7	0.3	2.8	3.1	0.90	–	>50
P-066	alp	9.9	1.3	2.7	7.2	0.38	–	>50
P-086	alp	10.6	1.5	2.5	7.9	0.32	129	10-50
P-076	alp	8.6	1.1	2.5	5.7	0.44	–	10-50
P-080	alp	9.5	1.2	2.3	7.9	0.29	734	10-50
P-078	alp	8.9	1.2	2.2	6.6	0.33	403	>50
P-055	alp	10.6	1.4	2.2	7.8	0.28	–	10-50
P-072	alp	11.1	1.7	2.2	9.2	0.24	–	10-50
P-074	alp	6.9	1.0	2.1	3.9	0.54	–	10-50
P-075	alp	9.0	1.3	2.1	7.0	0.30	–	10-50
P-071	alp	8.4	1.1	2.1	6.3	0.33	–	>50
P-097	alp	9.2	1.3	2.0	6.7	0.30	551	10-50
P-085	alp	8.3	1.1	2.0	7.2	0.28	492	10-50
P-022	alp	7.9	1.0	1.8	6.7	0.27	445	10-50
P-060	alp	8.8	1.3	1.8	6.5	0.28	–	>50
P-082	alp	8.4	1.2	1.8	8.3	0.22	–	10-50
P-024	alp	9.9	1.4	1.7	8.3	0.20	62	10-50
P-096	alp	6.8	0.9	1.6	5.8	0.28	486	10-50
P-049	alp	8.1	1.1	1.3	6.6	0.20	–	10-50
P-098	es	9.4	1.4	1.8	6.4	0.28	490	10-50
P-095	es	7.3	0.9	1.7	5.9	0.29	349	10-50
P-031	lbg	11.0	1.3	3.8	7.8	0.49	–	>50
P-032	lbg	9.7	1.3	2.4	8.4	0.29	–	>50
P-003	lbm	9.2	1.0	3.6	6.9	0.52	503	>50
P-027	lbm	12.4	1.7	3.6	7.7	0.47	–	>50
P-029	lbm	10.0	1.0	3.5	7.5	0.47	–	>50
P-015	lbm	9.9	1.3	3.2	7.7	0.42	237	>50

***Table A-4** (continued)*

Sample Number	Geologic Unit	Total Counts (ppm)	eK (%)	eU (ppm)	eTh (ppm)	eU/eTh	Soil Gas Rn (pCi/L)	Ground-Water Depth (ft)
P-017	lbm	9.4	0.9	3.1	6.4	0.48	314	10-50
P-057	lbm	10.1	1.0	2.9	10.2	0.28	580	>50
P-025	lbm	8.2	1.0	2.4	6.2	0.39	229	10-50
P-064	lbm	7.7	1.0	2.4	5.9	0.41	–	>50
P-004	lbm	10.2	1.3	2.3	8.0	0.29	884	10-50
P-090	lbm	8.1	1.2	2.1	5.4	0.39	–	10-50
P-069	lbm	–	–	–	–	–	1463	10-50
P-063	lbs	12.3	1.5	3.4	10.7	0.32	158	>50
P-042	lbs	11.3	1.5	3.4	7.6	0.45	–	>50
P-040	lbs	13.9	1.6	3.4	12.2	0.28	–	<10
P-043	lbs	9.5	1.2	3.0	5.8	0.52	–	>50
P-028	lbs	8.6	1.0	2.9	5.7	0.51	–	>50
P-045	lbs	10.0	1.1	2.5	8.1	0.31	207	>50
P-014	lbs	11.3	1.6	2.4	10.0	0.24	97	>50
P-081	lbs	10.8	1.6	1.6	10.2	0.16	–	>50
P-088	lbs	6.9	0.8	1.5	6.9	0.22	–	>50
P-018	lpd	7.5	0.9	2.2	6.6	0.33	175	10-50
P-008	lpd	9.1	1.2	2.0	6.4	0.31	205	10-50
P-094	lpg	8.4	1.1	2.4	6.3	0.38	420	10-50
P-087	lpg	8.0	1.1	2.1	6.1	0.34	349	10-50
P-100	lpg	6.7	1.0	1.2	4.4	0.27	–	10-50
P-053	lps	10.3	1.1	2.9	6.9	0.42	106	10-50
P-006	lps	9.7	1.2	2.5	7.0	0.36	619	10-50
P-009	lps	9.2	1.2	2.3	5.6	0.41	513	<10
P-077	lps	7.6	0.9	1.6	6.4	0.25	447	10-50